NTNU

Norwegian University of
Science and Technology

Aspects of Hydrate Management

Deposition Phenomena

Heidi Langen

Petroleum Geoscience and Engineering
Submission date: June 2016
Supervisor: Roar Larsen, IPT

Norwegian University of Science and Technology
Department of Petroleum Engineering and Applied Geophysics

Acknowledgement

I would like to thank my supervisor Roar Larsen for very good counseling and guidance throughout the work with this thesis. His knowledge on the subject and the advices given for this task has had a large impact on the quality of the results. I would like to show my great appreciation to Frank Ormøy at SINTEF Petroleum Flerfase for invaluable assistance with creating, assembling and adjusting the different equipment needed for the experiments done in this work, in spite of limited resources. I also appreciate the way the other employees at SINTEF Petroleum Flerfase have welcomed me to their workplace to do my experiments, the interest they have showed for my work and the suggestions they have expressed to improve it. In addition to this, I would like to thank my family, friends and fellow students for the encouragement and support they have given my through the entire study period.

Abstract

The purpose of this thesis has been to investigate the factors with the largest influence on the adhesion strength of a hydrate deposit on a solid surface. This has been done through a literature study on the subject, and a thorough experimental project in a laboratory. The experiments involved forming hydrate deposits on a pipe of steel, before removing the deposits and finding the pressure required to do so. The hydrate was formed by a solution of tetrahydrofuran and water in a tank where the pipe was submerged. The system achieved hydrate-forming conditions by flowing cold fluid through the pipe. After hydrate had deposited at the pipe surface, it was first left to grow for a certain time before a scraping device was pushed down the outside of the pipe with the use of a pump attached to a piston. The scraper removed some of the hydrate deposit, and a manometer measured the pressure provided by the pump at this point.

The experiments involved five different cases; one with ice deposits and four with hydrate. The one with ice was performed by using a pipe with relatively high surface roughness. The four hydrate cases involved one with the same high roughness pipe, one with a smoother pipe, one with the rough pipe coated with automotive paint and the last was with the smooth pipe coated with a primer originally used to avoid corrosion. Each case was tested at two temperatures and three to four different no-touch times. The parameters tested in the lab were temperature, growth time of the hydrate layer (no-touch time), thickness of the layer and the surface roughness of the solid surface. The last two parameters were found to have the largest impact, but the two others also had some significance. The lowest tested temperatures gave higher pressure readings than the ones with high temperature. A smooth surface resulted in lower adhesion than when the roughness was higher. The thickness of the deposit had a close to proportional relationship with the pressure, i.e. a thick layer resulted in strong adhesion to the surface. Thick layers usually occurred at long no-touch times, meaning that the longest no-touch times also gave strong adhesion.

Sammendrag

Arbeidet i denne oppgaven er gjort for å undersøke faktorene som har størst innflytelse på adhesjonsstyrken til en hydratavsetning på en fast overflate. Dette er blitt gjort gjennom en litteraturstudie av noe av det som finnes om emnet, og et grundig eksperimentelt prosjekt i laboratoriet. Eksperimentene innebar å danne hydratavsetninger på et rør av stål, for så å skrape dem av og finne det nødvendige trykket for å gjøre det. Hydratet ble dannet av en blanding av tetrahydrofuran og vann i et kar der et stålrør var nedsunket. Systemet oppnådde betingelsene for å danne hydrat ved at kald væske strømmet gjennom røret. Etter at hydrat hadde blitt avsatt på røroverflaten, fikk det først en hvis tid til å vokse før et skrape-verktøy ble dyttet nedover på utsiden av røret ved hjelp av en pumpe festet til et stempel. Skraperen fjernet noe av hydratavsetningen, og et manometer målte trykket som pumpen leverte ved dette punktet.

Eksperimentene innebar fem ulike tilfeller; én med avsetning av is og fire med hydrat. Testene med is ble gjort med et rør med relativt høy overflateruhet. De fire med hydrat involverte ett med det samme ru røret, ett med et glattere rør, ett hvor det ru røret var dekket med billakk og det siste med det glatte røret dekket med ruststopp grunning. Hvert tilfelle ble testet ved to temperaturer og tre til fire forskjellige vente-tider. Parameterne som ble testet i laben var temperatur, veksttid, tykkelse på laget og overflateruheten til den faste overflaten. De to siste av disse ble funnet til å ha størst innvirkning, men de to andre var heller ikke uten betydning. De laveste temperaturene ga høyere trykkavlesning enn eksperimentene ved høy temperatur. En glatt overflate ga lavere adhesjonskraft enn ved større ruhet. Tykkelsen til avsetningen hadde et tilnærmet proporsjonalt forhold med trykket, et tykt lag ga altså sterk adhesjon til overflaten. Lange ventetider ga vanligvis tykke avsetningslag som igjen ga høyt trykk ved fjerning av laget.

Table of Contents

List of Figures

List of Tables

Introduction

Gas hydrate is one of the major flow assurance challenges in production of petroleum, and avoidance of it accounts for a significant portion of the operational costs in a field. The most common practice is to take actions to avoid hydrate formation completely, since removal of it can be expensive, time demanding and dangerous. One can however never be 100 % safe from hydrate formation, as dysfunctions in the hydrate control systems may occur. Any hydrate formation needs to be detected as soon as possible, so actions can be made to avoid it from making large plugs that fully clogs the pipe. Hydrate inside a pipe can be both floating in the liquid stream as particles or larger lumps, or it can deposit on the pipe walls and thereby decrease the area where the fluids can flow through. This thesis focuses on the last case.

The main purpose is to find what parameters have the largest influence on how easy or difficult it is to remove a hydrate deposit from a solid surface, i.e. the adhesion force of the hydrate. Some literature on the subject will be investigated, involving work done on hydrate adhesion and more general subjects like wettability, interfacial tension, adhesion and roughness. An experimental study will also be done, where different aspects of this topic are tested. The desired outcome is that this work can increase the knowledge about *how* hydrate deposits to a surface, and what factors play a role in how *strongly* it attaches to the surface. The most likely application of the findings is within the petroleum industry, more precisely production lines and other equipment where the risk of hydrate formation is substantial. In practice this may mean that the materials or coatings used as the inner surface of such equipment is adjusted based on the results, so that it is more difficult for any hydrate to "stick" to the surface, and possible hydrate deposits will also be easier to remove due to low adhesive forces.

1 Theory

1.1 Hydrates

In a petroleum-producing pipeline, one of the most challenging and dangerous problems that can occur is formation of gas hydrate. Gas hydrate has similarities to ice, but the main difference is that light, natural gas molecules are trapped inside the crystalline structure of the water molecules, and the structure itself is also different (Sloan & Koh, 2008, p.1). Hydrate can have several different structures, but the most common occurring in petroleum production is called structure II or just sII. For gas hydrate to be formed, four main criteria need to be met. These are the presence of water, light gas molecules, high pressure and low temperature. The cavities that occur inside of the crystalline structure of water are relatively small, and this is the reason why small and light gases are the most common "guest molecules" in gas hydrate. All of the cavities in the hydrate do not need to be filled with gas, but the higher percentage that is filled, the more stable the hydrate will be. An example of the molecular structure of hydrate is shown in Figure 1.1.

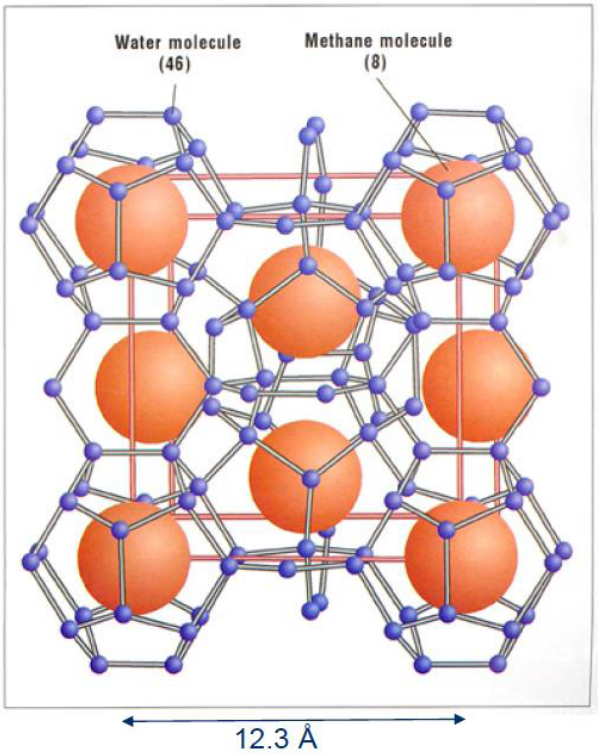

Figure 1.1: Molecular structure of methane hydrate (Larsen, 2014)

The phenomenon of gas hydrate was first discovered around 1810 by Sir Humphrey Davy, and it was recognized as a problem in producing petroleum pipelines in 1934 by E. G. Hammerschmidt (Sloan & Koh, 2008, pp.1-5). Ever since this discovery, gas hydrate has been one of the main concerns regarding flow assurance in the petroleum industry. The most widely used method to control this problem is injection of thermodynamic hydrate inhibitors (THI), like methanol and monoethylene glycol (MEG). THIs have traditionally been injected at such a high rate that hydrate formation can be completely avoided, and this is still the main practice. The problem is that this consumes tremendous amounts of chemicals that may cause

environmental harm if released to nature, and it also accounts for a significant part of the operational costs (Usman et al., 2012). Due to this, a lot of research and money has been used to explore different methods of hydrate management. In hydrate management, the operational properties (pressure and temperature) are allowed to carefully enter the hydrate formation zone with constant monitoring and several precautions taken beforehand. Some hydrate may be formed in the pipeline, but it is not allowed to grow at a high rate possibly leading to hydrate plugging. Some of these methods will be discussed more in detail later.

1.2 Hydrates Versus Ice

As mentioned above, gas hydrate has some distinct similarities to ice. Some of the major reasons are that both have crystalline structures and that the main component is water (Sloan & Koh, 2008, Ch.2). There are other similarities as well, and this gives the opportunity to use knowledge from experiments and other literature with ice when working with hydrate, since the knowledge of hydrate is very limited compared to that of ice. If however knowledge from ice is used when working with hydrate, one needs to be aware of the differences between them as well. Two of the most inconspicuous differences is that the cavities in hydrate are filled with light gas molecules like methane, ethane, propane and carbon dioxide, and the fact that hydrate usually needs higher pressure than ice to be formed. Hydrate does also have a higher melting point than ice, meaning that hydrate can be formed at temperatures above zero degrees Celsius. Some other physical properties that are different are the length of the hydrogen bonds, the diffusivity time, reorienting rate, elasticity and thermal conductivity. Hydrates have a bit longer hydrogen bonds, making the angle between the oxygen-molecules different. The diffusivity time for water molecules in hydrate is twice the time in ice, and the reorienting time for the water molecules is half of that for ice. This might be the explanation that the resistance against creep is higher for hydrate than ice. When it comes to the elasticity, it has been found that the elasticity for methane hydrate is almost isotropic, while there is a significant anisotropy for ice. The thermal conductivity for hydrate is lower than that for ice, and the thermal conductivity for tetrahydrofuran hydrate is found to have proportionality with temperature, but is independent of pressure (Sloan & Koh, 2008, Ch.2).

Aspenes et al. (2010) states that ice and hydrate has fairly similar behavior when it comes to adhesion. For ice it is found that both particle size and contact time is proportional with the adhesion force occurring between two ice particles, and there is reason to believe that this is also the case for hydrate. Experiments performed by Aman (2012, p.42) have proven this to be true for hydrate; contact time is proportional with adhesion force, but only within a certain time frame. The adhesion forces increases for a period of time, but then it stagnates and hydrate *growth* may (or may not) become the dominant mechanism.

Liukkonen et al. (1997) did experiments to investigate the adhesion between oil and ice, both with and without liquid water present. These experiments are explained more in detail in the chapter on wetting. The conclusion from this work was that the adhesion between oil and ice was much stronger when air was the surrounding fluid compared to when it was liquid water. With water present, the oil drop spread to a very little extent on the ice surface and it started moving along the surface at a low inclination angle, meaning that the adhesion was weak. Without liquid water, the oil drop spread to an extent where it was difficult to

measure the contact angle, and the adhesion was relatively strong. If the ice in the experiments instead were replaced with hydrate, the conclusion would not necessarily be the same. Aspenes et al. (2010) found that the adhesion force between two hydrate particles or one hydrate particle and a solid surface increased significantly if there was liquid water present. The increase could be as much as an order of magnitude, and this was due to the mechanism of liquid bridging, which will be explained later. The experiments of Aspenes et al. do however not include anything on the adhesion between hydrate and oil, so no wider conclusion can be drawn based on the basis of the two papers mentioned here.

1.3 Hydrate Deposition

Deposition of hydrate on the inside of production pipes is a large flow assurance problem. The deposited hydrate decreases the diameter of the pipe and this leads to a change in the flow rate and pressure of the fluid flowing through it. The flow regime may also change, causing a significant change of the conditions for the whole production system. The decrease in pipe diameter may also lead to a Joule-Thomson expansion of the gas where the diameter returns to the original one, decreasing the gas temperature. According to Aspenes et al. (2010), hydrate deposition in a producing pipe is affected by the surface of the inside of the pipe, the composition and properties of the fluids in the pipe and the amount of water present (water cut). The velocity of the fluid flow has also been shown to be of some importance.

Aspenes et al. (2010) states that the contact time is of significant importance when it comes to adhesion force between two ice particles, and this is most likely also applicable for two hydrate particles and a hydrate particle and a solid surface. A long contact time leads to a high adhesive force, so if one would want to avoid deposition, the contact time should be decreased to a minimum. This could be done by increasing the fluid velocity, and Nicholas et al. (2009) did some experiments on this. When petroleum fluid flows through a pipeline, the flow is usually assumed to be turbulent. The exception is the boundary layer occurring right up to the pipe wall, which in most cases is laminar. It is at this location that hydrate deposition occurs, so the mechanism of laminar flow needs to be taken into consideration. Nicholas and coworkers conducted experiments with cyclopentane hydrate and a steel pipe investigating the impact of the fluid velocity and particle size regarding removal of already deposited hydrate on the steel. It was found that there is a relatively strong correlation between the size of the deposited particle and the velocity needed to remove the particle. As the size of the particle increase, the required velocity to remove it decreases, and thus there is an inverse proportionality between the two parameters. As an example, a particle with a diameter of 2 microns will be removed at a velocity of 2.3 m/s, while a particle with a diameter of 5 microns only needs a velocity of 1.5 m/s to be removed. It was concluded that all particles with a diameter equal to or above 3 microns would be removed under so-called normal operations, while the smaller particles need higher velocity. Figure 1.2 shows the relationship between the particle diameter, removal velocity and dimensionless height. The dimensionless height is a relative parameter that can be used to see if the deposited particle is within the laminar boundary layer or not. The laminar boundary layer is defined where the dimensionless height is below 30. As seen from the figure, the majority of the tested particle diameters are within this dimensionless height range.

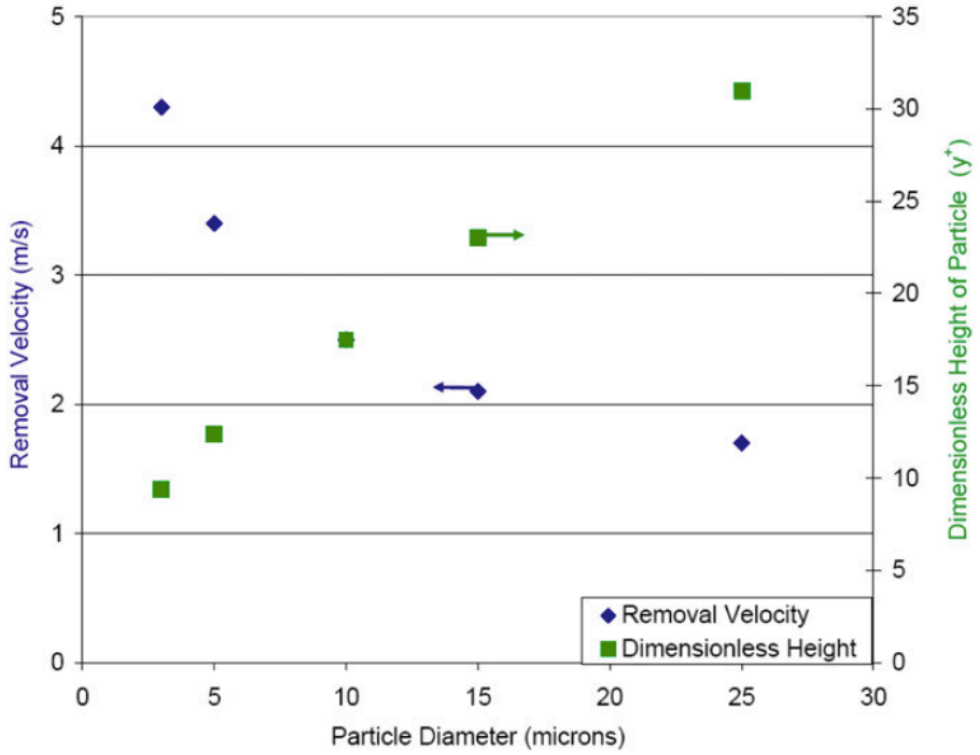

Figure 1.2: Particle diameter of deposited THF hydrate particle on carbon steel versus removal velocity (left ordinate) and dimensionless height (right ordinate) for a methane system (Nicholas et al., 2009)

The results from the work of Nicholas et al. gave the conclusion that the velocity to remove a deposited hydrate particle was not very large, meaning that a fluid flow with this velocity may prevent hydrate particles from depositing on the surface in the first place. The team therefore made further investigations to see if no hydrate deposition during normal operations was really the case. The hypothesis that hydrate particles emulsified in the flowing fluid does not deposit on the pipe wall may be more or less accurate, but another possible mechanism must also be taken into consideration. The pipewall is in fact in most cases the coldest location in the flowline system, making it a suitable location for hydrate formation. So even if hydrate particles does not to a large extent *deposit* on the pipe wall, it may actually be *formed* there. If this is the case, the adhesion force has been found to be much larger than if the hydrate particle is deposited. The adhesive force is especially strong if there is liquid water present, as will be explained in more detail later in this thesis. Hydrate particles formed at the pipewall are thus more difficult to remove, and if not removed, the hydrate may easily grow in volume and strength on the wall, increasing the problem drastically as mentioned earlier. Figure 1.3 shows what happens if there already is a layer of hydrate deposited on a solid surface and a hydrate particle is suspended in the surrounding fluid. The hydrate particle is wetted with water, and is quickly absorbed to the hydrate layer, making it grow larger.

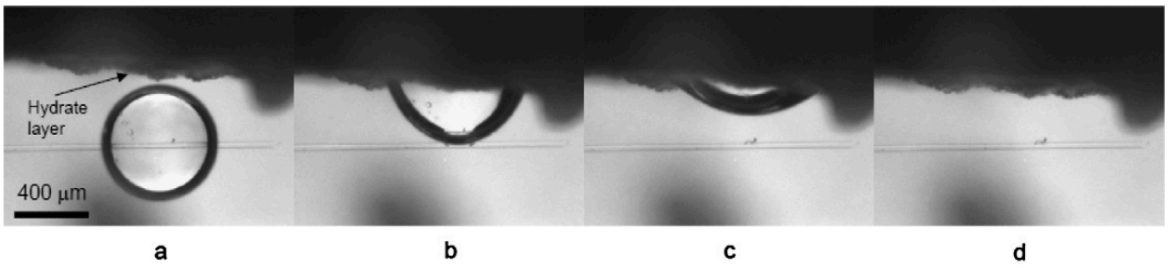

Figure 1.3: Water-wet THF hydrate particle being brought in contact with a layer of hydrate deposited on a steel surface. The absorption of the hydrate particle is shown through the pictures a-d, which are all taken less than a second apart (Nicholas et al., 2009)

1.4 Hydrate Control Methods

There are two categories regarding hydrate control. These are hydrate avoidance and hydrate management, where the first operates outside of the hydrate formation zone and does not allow any hydrate to form, while the other is opposite. Hydrate management requires a higher level of caution and leads to a larger risk, but it may also lead to a significant cost saving. Figure 1.4 shows most of the different hydrate control methods, where the most common methods are the thermal and chemical ones.

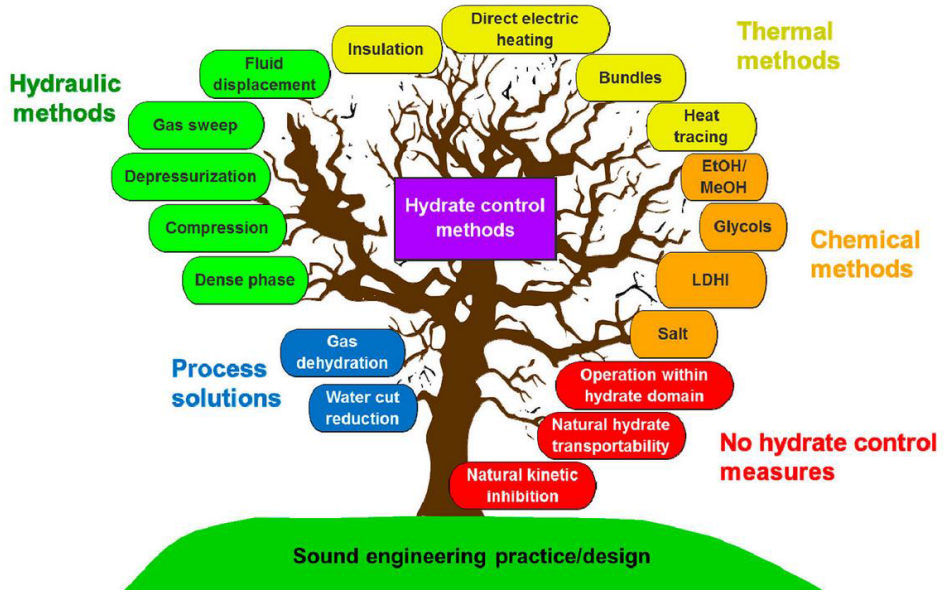

Figure 1.4: Most of the hydrate control methods used at different extents today (Kinnari et al., 2014)

As mentioned earlier, the most widely used hydrate control method is injection of thermodynamic hydrate inhibitors (THI). The way these work is that they displace the hydrate equilibrium curve to conditions of lower temperature and higher pressure, so that the system can operate at conditions that originally were inside of the hydrate formation zone. This is shown in Figure 1.5. Here it is seen that without any methanol, hydrate may form when the rightmost line is crossed. Adding methanol to the system shifts the line to the left, and it is possible to operate at lower temperature and higher pressure.

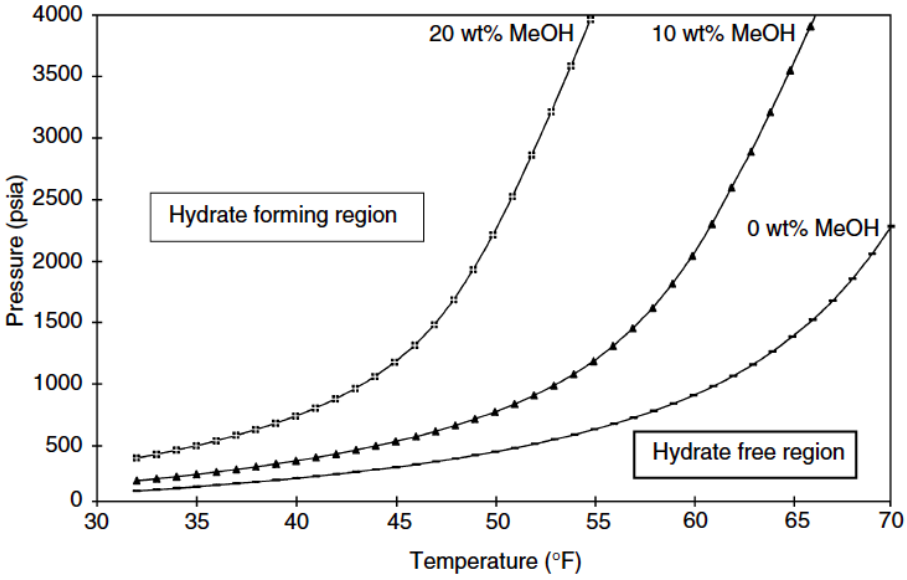

Figure 1.5: The phenomena of adding methanol to a gas system (Sloan & Koh, 2008, p.647)

A hydrate management method similar to THI is *underinhibition*, where the amount of inhibitor used is less than what is needed for complete hydrate avoidance. Some hydrate may be formed in the system, but the fraction is too small for it to turn into large lumps and possible plugs. A significant amount of chemicals will be saved with this method, reducing both the environmental impact and the operational costs. The method is however not very widely used due to the increased risk, as a full avoidance of hydrate formation is still the most common practice. This means that an underinhibition in the system is most often considered a problem and an indication that something is wrong regarding the inhibition system.

Another method involving injection of chemicals is using low dosage hydrate inhibitors (LDHI). With these inhibitors, a much smaller amount of chemical is needed compared to THIs, usually just about 0.5-2 wt% where THIs need 40-60 wt% (Sloan & Koh, 2008, pp. 659-669). There are basically two types of LDHIs; kinetic hydrate inhibitor (KI) and anti-agglomerant (AA). KIs avoid hydrate formation by hindering hydrate nucleuses from reaching the critical radius needed to start growing into a hydrate particle. KIs can only delay the start of hydrate growth, if all of the KI molecules are "used", hydrate growth will happen in the same way and at the same rate as if there were no hydrate control at all. Anti-agglomerants work at a later stage in the hydrate growth process. Hydrate particles are allowed to form, but the AA denies the particles from sticking to each other, and a flowable slurry of hydrate flows as a dispersion in the other fluids in the system.

A hydrate control method very widely used, is insulation of the pipeline (Aarseth, 1997). This involves covering the steel pipe with some type of insulating material, leading to a better temperature maintenance of the fluids flowing inside the pipe. In offshore installations, the pipe lying on the seafloor is often exposed to temperatures below 10 °C, and this is in most cases within the hydrate formation zone. The fluid flowing from the petroleum reservoir is hot and far from entering the hydrate formation area, but when it reaches the wellhead and the pipeline at the seabed, it will cool rapidly if the pipe is uninsulated. A well-insulated pipe can maintain a large amount of the heat from the fluid, and keeps the system outside of the hydrate zone.

1.5 Adhesion & Cohesion

There are two different ways a solid particle can attach to something, and what it attaches to, defines what this is called (Aman, 2012, Ch.1.5). If for example a hydrate particle attaches to another hydrate particle, it is called *cohesion.* If on the other hand the particle attaches to a solid surface like a pipewall or a sample of glass, it is called *adhesion.* Generically speaking, cohesion forces between two similar particles are stronger than the adhesion force between the same particle and a solid surface. Aspenes et al. (2010) found that the cohesive force between cyclopentane hydrate particles was almost an order of magnitude larger than the same force between a hydrate particle and the solid surfaces tested in their experiments. The solid surfaces tested in these experiments were carbon steel, stainless steel, aluminum, brass, glass and a surface with an epoxy coating. The surfaces have different surface free energy, and it was found that surface free energy is proportional with solid-hydrate adhesion force. Out of the six surfaces, glass had the highest surface free energy and therefore the highest adhesion force regarding a cyclopentane hydrate particle, as seen in Figure 1.6.

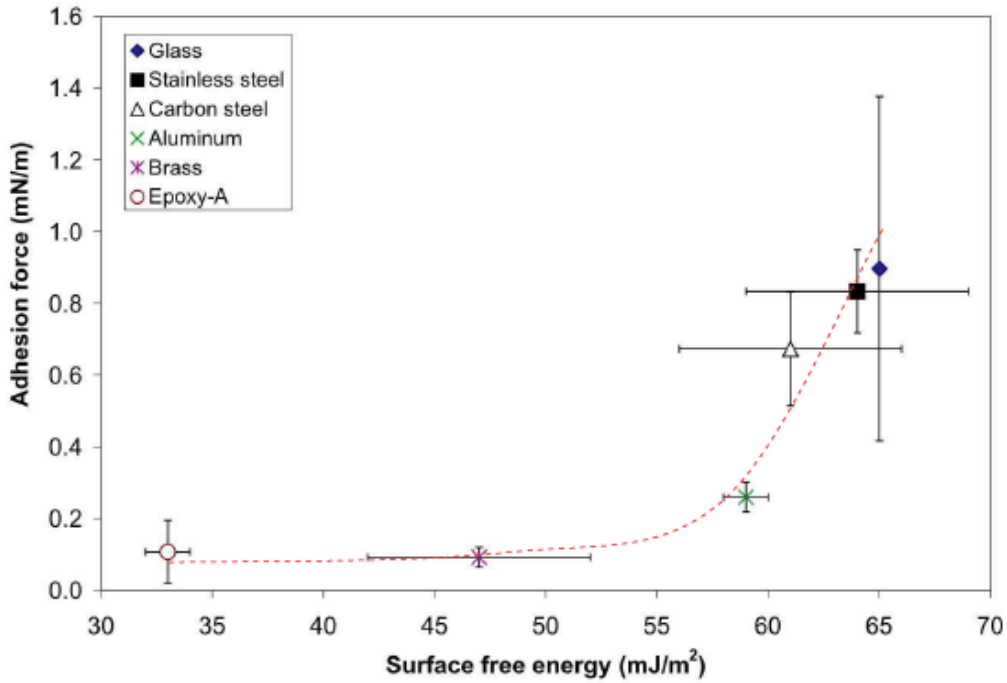

Figure 1.6: Surface free energy versus adhesion force between different solid surfaces and a cyclopentane hydrate particle (Aspenes et al., 2010)

Aspenes et al. (2010) also did experiments where acid and water were added to the system. Both experiments with acid alone, water alone and both acid *and* water were performed. Adding acid to the system led to a significant decrease in the adhesive forces. A possible explanation for this is that the acid is adsorbed to one or multiple of the surfaces in the system, and thereby hinders the other substances from sticking to each other. The adhesive force between all of the solid surfaces and a hydrate particle, and between two hydrate particles *with* acid present was much lower than for the corresponding systems *without* acid. The force between a hydrate particle and a solid surface with acid was in fact so low that it was difficult to measure. The impact of acid on the adhesive force is shown in the figure below.

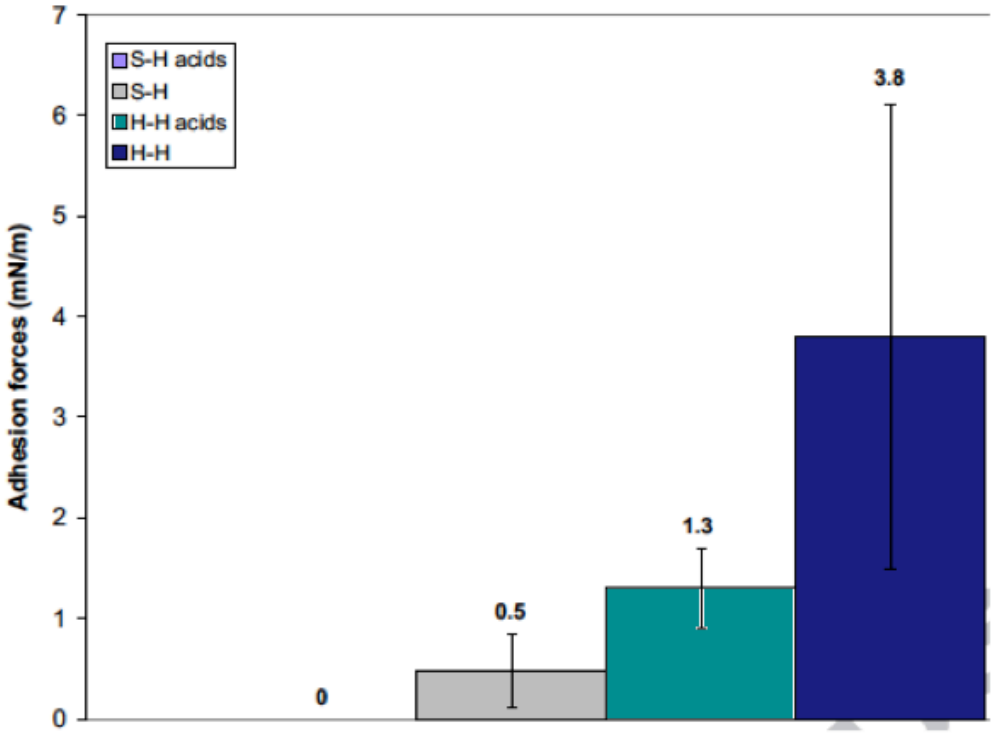

Figure 1.7: Impact on adhesive forces when adding acids to the system, between solid surface and hydrate particle (S-H) and between two hydrate particles (H-H) (Aspenes et al., 2010)

The experiments where water was added to the system gave almost the complete opposite results than the ones with acid. Presence of water increased the adhesive force between two hydrate particles by an order of magnitude, and the forces between the solid surfaces and a hydrate particle did also increase significantly. The reason for this is that water works as a liquid bridge between the two substances in question and therefore makes them stick to each other more efficiently than without this bridge. Liquid bridging will be explained more in detail later. Another possible explanation is that with water present, hydrate can be formed at a higher rate as water is one of the criteria for hydrate growth. A larger volume of hydrate may cause higher adhesive forces, and it is difficult to divide the two mechanisms (liquid bridging and growth) to find the one with the largest impact.

Combining both acid and water into the system would show which of the effects are more dominant. Acid reduces adhesive forces, while water increases them. It was found that with both water and acid, the adhesive force between two hydrate particles was about the same as the force with no water and acid. Comparing the results from experiments between hydrate particles without any other substance, with acid, with water and with both acid and water is shown in Figure 1.8. This shows that adding just water gives the highest adhesive force, just acid gives the lowest, and the two other are somewhere between with a similar result.

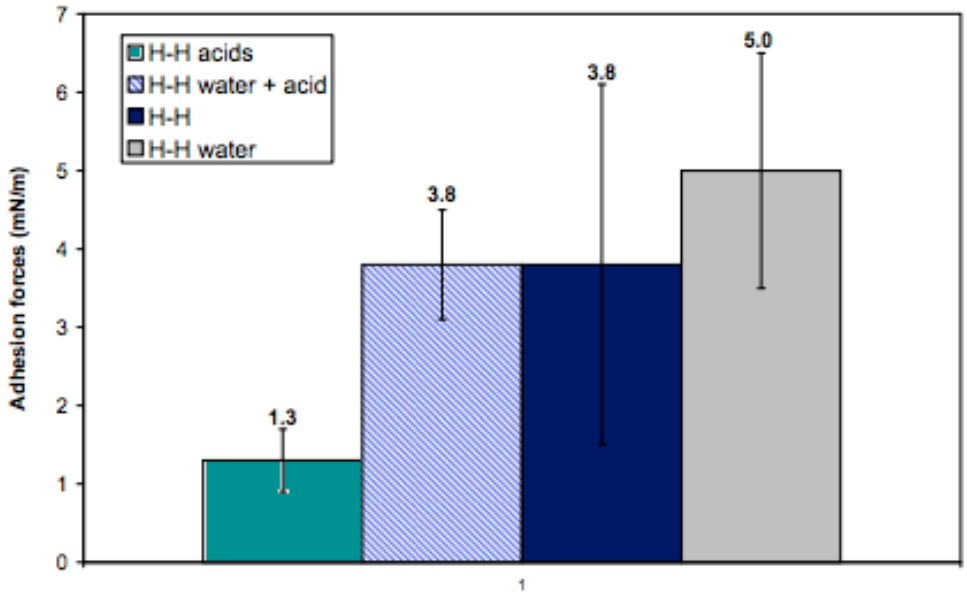

Figure 1.8: Comparison of adhesive forces between hydrate particles alone (H-H), with adding water (H-H water), acid (H-H acid) and both water and acid (H-H water + acid) (Aspenes et al. 2010)

Baraka-Lokmane et al. (2014) did experiments to investigate what type of coating would reduce scaling on a subsurface safety valve, and also what parameters had the largest influence on this. The experiments were not done with hydrate as the depositing substance, but carbonate, sulphate and sulphide scale, which can also cause large flow assurance problems. The work done by Baraka-Lokmane et al. included twenty different coatings, originating from seven different chemical categories. These categories included fluoropolymers, textured hydrophobic paint and diamond-like carbon, among others. The authors state three important facts on the subject of their work. The first of these is that the properties of the solid surface in question plays an important role regarding scaling on it. The most important properties are the roughness and the micro- and nanostructuring that occur when the wettability of the surface changes. The second fact stated is that the surface deposition kinetics has a large influence. There is a connection between the time constant for bulk and surface deposition, but it is not clear if this correlation is valid in all flow environments. The third fact concerns the induction time for scaling. Even when the conditions for scaling are present, it may not occur spontaneously as soon as these conditions arise. Whether or not, and if so, when, scaling is initiated, is influenced by the flow regime, saturation rate and also the surface parameters of the system. An example that proves this is the well-known fact that if a surface already has a layer of scale – either thin or thick – additional scaling or deposition will occur much faster and to a larger extent than on a completely clean surface. In other words, in a system where any scale has yet to be made, some sort of barrier needs to be overcome before scaling is initiated.

Baraka-Lokmane et al. also mention three different mechanisms where scale may form. All of these involve situations where the solubility of the salt(s) present in the system decreases, so precipitation and hence scale is very likely to happen. The experiments done by Baraka-Lokmane et al. were conducted with a standard bulk jar test with a rotating cylinder electrode (RCE) installed. The purpose of a RCE is to have the possibility of changing the

flow conditions so both laminar and turbulent flow can be tested while the other parameters are the same. As mentioned above, flow conditions like fluid velocity and movements in the bulk can have a large influence on whether or not and to what extent scaling occurs. Based on this, several different flow conditions, both within laminar and turbulent flow, were tested.

The results from the experiments with carbonate and sulphate scale showed large differences, both among the different coatings and between laminar and turbulent flow conditions. In laminar flow, the coating made of unmodified nickel alloy gave by far the largest layer of scale with a mass gain of 12.0 ± 2.5 mg. These experiments did not show any clear relationship between the chemical properties of the coatings and the extent of scaling on the specific coatings. In turbulent flow however, the amount of scaling was much higher for some of the surfaces, and it was possible to identify some connections. The largest mass gain seen here was for the fluoro-polymer coating with a gain of 40.1 ± 8.3 mg. It was found that the flow rate is of large importance regarding the degree of scaling, and in many cases, it actually exists a linear relationship between the scaling growth and the Reynolds number.

With the use of a scanning electron microscopy (SEM), Baraka-Lokmane et al. found some interesting relationships between the coatings having good anti-scaling properties and those who didn't. The crystals of scale made on the surfaces with low mass gain were very small, while the others had significantly larger crystals growing out of the surfaces. This showed that the high performing anti-scale coatings were able to prevent or delay scaling nucleation on the surface, meaning that the nucleation is implemented at a later time and therefore the crystals have less time to grow. The difference in the crystal size between the good and the poor anti-scaling surfaces are shown in Figure 1.9.

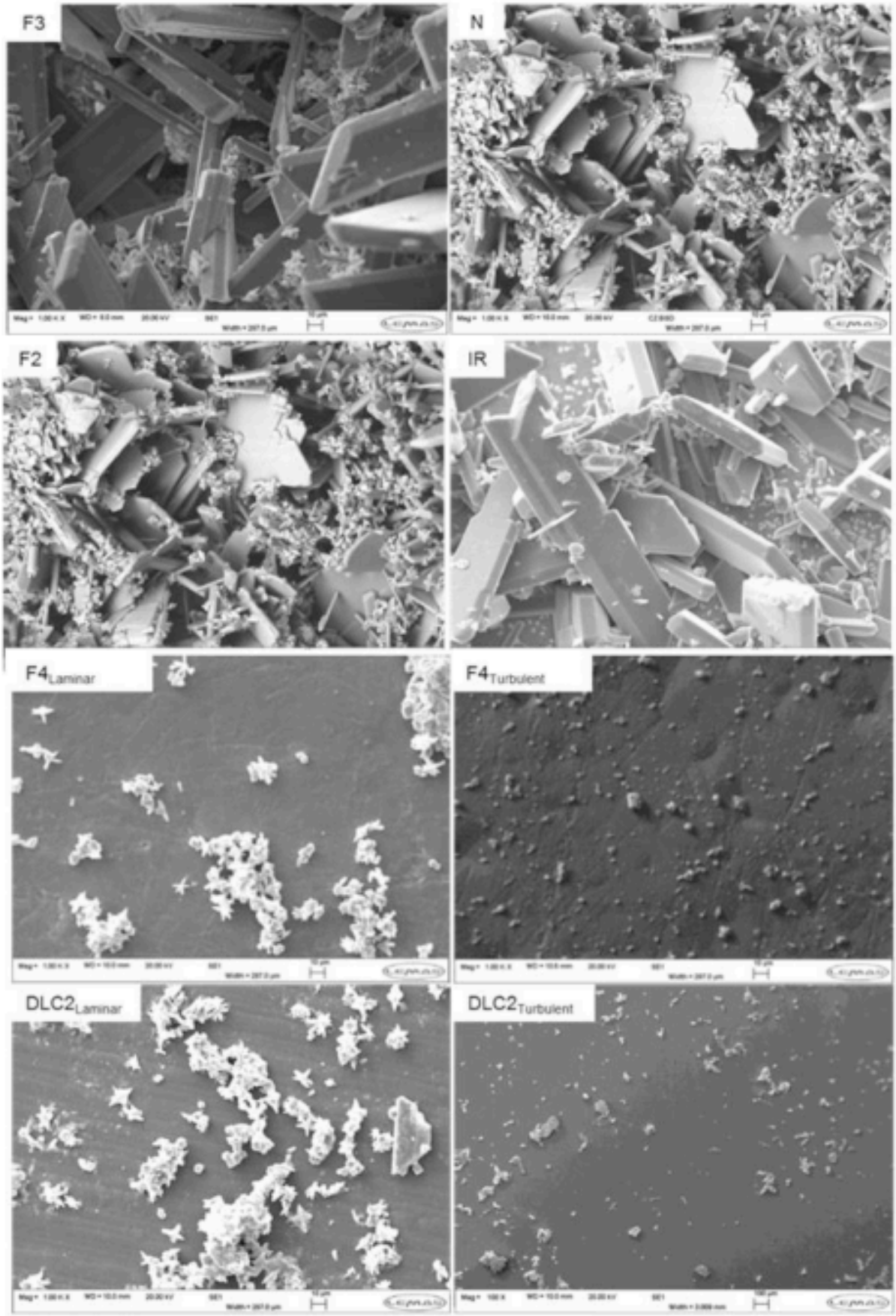

Figure 1.9: Difference in crystal size between poor anti-scaling surfaces (top four pictures) and good anti-scaling surfaces (bottom four) (Baraka-Lokmane et al., 2014)

The results from the experiments with sulphide scale were quite different from the two other tested substances. As explained above, there were large differences between laminar and turbulent flow conditions in the carbonate and sulphate scale experiments. In the sulphide scale experiments however, the mass gain was relatively similar between the two flow conditions, and several surfaces even gave somewhat lower mass gain in turbulent flow than in laminar. A possible explanation for this is that surface adhesion is the primary mechanism for the surface fouling, instead of surface nucleation and growth as in other cases. This is due to the very low solubility products of zinc sulphide and lead sulphide, leading to a high possibility for these salts to precipitate in the bulk instead of nucleating on the surface. The scale particles in the bulk will eventually adhere to the surface, but the adhesion force is lower than if the particles had been initially formed at the surface, meaning that a high fluid velocity can easily remove the scale from it.

The general findings from the work of Baraka-Lokmane et al. is that it is challenging to find clear relationships between the properties of a surface coating and its performance regarding anti-scaling. Their experiments did not show any clear proportionality between surface roughness and mass gain, or between surface energy and mass gain. They also found that the main cause of surface fouling is heterogeneous surface nucleation, and not direct adhesion, as many have believed. It is nevertheless important to note that surface roughness and surface energy is of some importance, but the connection between these and the mass gain is much more complex than a direct linearity and is therefore difficult to predict. An overall general rule of thumb is still that both low surface roughness and low surface energy will in most cases give a good anti-scaling surface.

1.6 Surface Free Energy & Interfacial Tension

The parameter surface free energy can be defined as "the work which has to be expended in order to increase the size of the surface of a phase" (Krüss, 2016). In other words, surface free energy is the amount of force any substance has to "use" to be able to spread out on a specific material. Surface free energy is given for the solid surface material, meaning that it has the same value independent of the substance trying to spread on it. The fact that different fluids spread to a different extent on the same surface has other explanation than this parameter, including the interfacial tension of the fluid, and wetting conditions of the system. The unit of surface free energy is given as either mJ/m^2 or mN/m, and as an example, glass has a surface free energy of 65 mJ/m^2 while epoxy-A has only 33 ± 1 mJ/m^2 (Aspenes et al. 2009a). Aspenes et al. (2010) found that surface free energy is proportional with adhesion force, i.e. a high surface free energy means that the force occurring between the solid surface and a fluid drop also is high. Using the example with glass and epoxy-A therefore gives a higher adhesion force for glass than for epoxy-A. This, together with the same result for four other solid surfaces, is shown in Figure 1.6. Aspenes et al. (2010) also found that the lower the surface free energy, the more probable the surface is to be oil-wet.

1.7 Wetting

Wetting in the context of petroleum states whether a surface "attracts" water or oil (Aspenes et al., 2009a). If water easily spreads on the surface, it is defined as *water-wet*, but if oil spreads more easily, the surface is *oil-wet.* There is also a possibility that the surface does not attract the one more than the other, this is called neutral or intermediate wetting. The wetting of a surface is usually defined and measured using the contact angle. This is the angle occurring between a water droplet and a solid surface when the droplet is placed on the surface, and the surrounding fluid is oil. A schematic of this is shown in Figure 1.10.

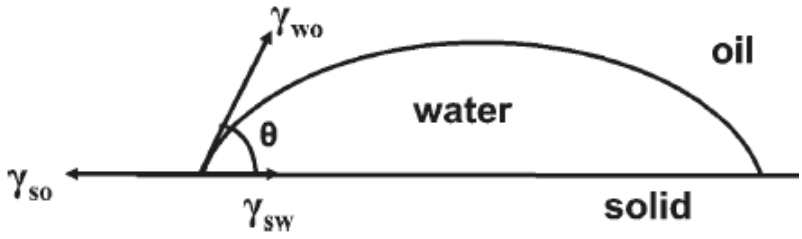

Figure 1.10: Figure showing how to measure the contact angle of water on a solid surface surrounded by oil (Aspenes et al., 2009a)

A common and fairly inaccurate way to classify wetting is to set a contact angle of 90° as a boundary point and say that angles below this represents water-wet surface, while angles above is oil-wet. A contact angle of exactly 90° is neutral wet. A more accurate way is to use three separate intervals of the contact angle from 0 to 180 degrees (Aspenes et al., 2009a). With this practice, 0° – 75° means the surface is water-wet, 75° – 105° is neutral or intermediate and 105° – 180° is oil-wet. The contact angle is a function of the different interfacial tensions in the system, shown in Figure 1.10. The equation that shows this relationship is called Young´s equation and is as follows:

$$\cos\theta = \frac{\gamma_{so} - \gamma_{sw}}{\gamma_{wo}} \tag{1}$$

where θ is the contact angle and γ_{so}, γ_{sw} and γ_{wo} is the interfacial tension between the solid and oil, solid and water and water and oil, respectively. The interfacial tension between water and oil combined with the contact angle provides an equation to find the adhesion force in the system, given below.

$$W_{swo} = \gamma_{wo}(1 + \cos\theta) \tag{2}$$

where W_{swo} is the adhesion force between the solid surface and the water drop surrounded by oil. From the equations above, it is clear that the interfacial tension of the different substances plays an important role regarding the adhesion between the substances in the system. Interfacial tension is an individual property, and varies from oil to oil, and solid surface to solid surface, and needs to be addressed beforehand in order to say anything about the adhesion and wetting of the system.

Aspenes et al. (2009a) did contact angle measurements on the same systems as described in Aspenes et al. 2010. Different oils were tested on the different surfaces, meaning

that the classification of wetting is the opposite of the one explained above, i.e. contact angles above 105 degrees are water-wet, while those below 75 degrees are oil-wet. There it was found that almost all of the surfaces were water-wet, nearly independent of the surface free energy. The exception was glass and to some extent stainless steel. The results from the experiments with two of the tested oils are shown in Figure 1.11.

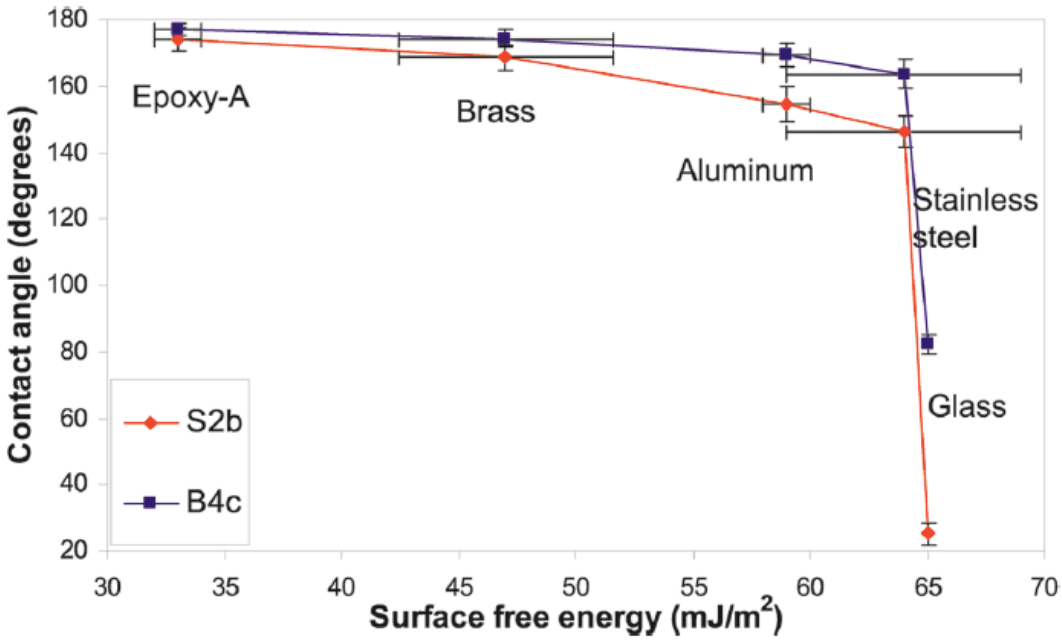

Figure 1.11: Contact angle versus surface free energy for five different solid surfaces and two different oils (Aspenes et al., 2009a)

From all of their different experiments, Aspenes et al. concluded that most of the common materials that may be used in a petroleum installation are initially water-wet. If and how strongly water-wet the surface is, depends on the solid surface material itself, and also on the composition of the fluids in the system. The pipeline wall is often the coldest location in a pipeline system, and if it at the same time is water-wet, hydrate may easily deposit or form on the pipewall given that the pressure and temperature is within the hydrate zone. Based on this, it can be very beneficial to find a material or coating that makes the pipewall less water-wet and therefore restricts hydrate formation on it. As explained under "Adhesion & Cohesion", the presence of acid reduced the adhesive force significantly. Aspens et al. found that acid in the system increased the contact angle, i.e. the surface became less water-wet.

Liukkonen et al. (1997) did experiments to investigate how and to what extent oil adheres to ice, both with and without liquid water present in the system. In the experiments without water present, a drop of oil was placed on the surface of an ice sample, and the initially horizontal piece of ice was slowly inclined. Inclination was continued until the drop of oil started moving or deforming downwards, and the inclination was stopped to measure the angle. In the experiments with water present, the procedure had to be different. Since oil has a lower density than water, the oil drop would just float to the water surface instead of adhering to the ice. Because of this, these experiments were performed by placing the oil drop underneath the ice sample submerged in liquid water. The ice sample would then be inclined slowly until the oil drop started moving upwards along the ice. Inclination was stopped and

the angle was measured. It was found that the two different systems gave very different results for the adhesion of oil on ice, meaning that liquid water has a large influence on this. The drop spread more easily (lower contact angle) on the ice in air than when liquid water was present, and the adhesion force between the oil drop and ice was about 20-30 times more in air than in water.

1.8 Heat Capacity

Heat capacity is a physical property referring to the amount of energy needed to raise the temperature of the specific substance by one degree (Celsius or Kelvin) (Tracy & Singh, n.d.). In other words, the heat capacity is the relationship between the change in temperature caused by adding or removing a certain amount of heat to/ from a material. Specific heat capacity is often also used in the same situations as heat capacity, the only difference between the parameters is that specific heat capacity is defined per unit mass, i.e. it defines the amount of heat needed to increase the temperature of one gram of the material by one degree. Heat capacity is individual for all materials, both solids and fluids, i.e. the heat capacity for wood is different than that for stainless steel as an example. This can easily be observed physically by touching these two materials at different temperatures. At a low temperature, the steel will feel much colder than the wood, even though they initially have the same temperature. Steel has a lower heat capacity, and it "steals" heat from the hand, making the surface feel colder than wood. Wood can maintain its own temperature to a higher extent, hence it feels warmer.

1.9 Roughness & Friction

The roughness of a solid surface may have a considerable impact on whether or not and to what extent another substance adheres to it. An example of this is placing a water droplet on a smooth glass plate and on a rough concrete floor. The drop on glass is much more easily removed compared to the one on concrete. Of course surface free energy and other properties of the materials play an important role in this experiment, but the roughness also has a large impact. A generic rule is that the smaller the roughness, the more difficult it is for a substance to adhere to it. Based on this, one may think that it is possible to avoid hydrate deposition on the pipewall if the roughness is eliminated or negligible, but it's not that simple. Making a completely smooth surface can be very expensive, and even if the surface is smooth at the time of installation, it will most likely change during the lifetime of the pipe. Together with water, oil and gas, the fluids flowing through the pipe also brings sand particles, wax, asphaltenes and acids that all may erode and grind the surface of the pipe and change the properties of it (Aspenes et al., 2009b).

Both Aman (2012, Ch.9.4) and Nicholas et al. (2009) did some experiments to investigate the impact of surface roughness on hydrate deposition. Aman tested four different roughnesses on samples of calcite, quartz and stainless steel. The different roughnesses were created by using an unmodified sample, and then treat three other samples with different grits of sandpaper. The unmodified – and therefore most rough – sample gave not surprisingly the highest hydrate adhesion force. What was a bit remarkable was that of the three modified samples, the one with the intermediate roughness gave the highest adhesion force, and hence

both higher and lower roughness gave less adhesion force. The result was most prominent on the quartz sample. The results of this experiment are shown in Figure 1.12 and Figure 1.13.

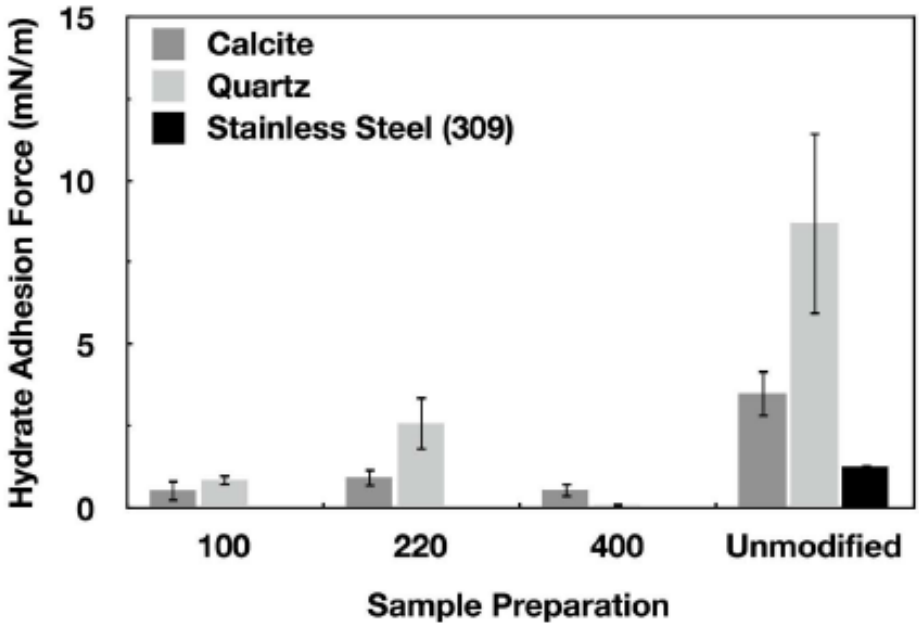

Figure 1.12: Impact of surface roughness on adhesion force. The numbers 100, 220 and 400 represents what grit of sandpaper is used to modify the roughness of the surface (Aman, 2012, p.158)

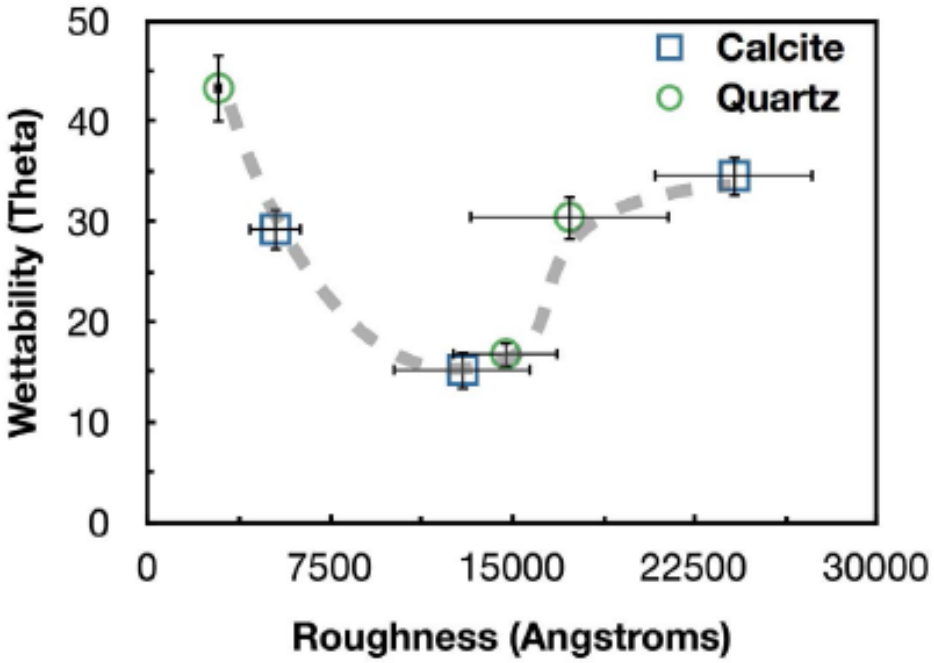

Figure 1.13: Impact of surface roughness on the wettability (contact angle) on calcite and quartz samples. Low roughness is equivalent to that a high number grit sandpaper (like 400-grit) has been used on the surface (Aman, 2012, p.159)

The experiments Nicholas et al. (2009) performed are less thorough than the ones done by Aman regarding roughness, since they only include two different roughnesses on carbon steel.

One sample was treated with diamond polish that made the roughness as small as 1 micron ($1\times10^{-6}m$), and the other sample was treated with 240-grit sandpaper, resulting in a roughness of about 59 microns. The experiments gave the conclusion that the roughness had no impact on the adhesive force between the sample and the hydrate particle. This is not in accordance with the results by Aman, but it may be due to the fact that it was a different material than in Amans experiments. It should also be mentioned that the span of the roughness in Amans work is smaller than the ones by Nicholas et al., up to 3 microns and 59 micron, respectively, and still the difference is larger in Amans experiments. Some of the results from the work of Nicholas et al. are seen in Figure 1.14. Tests were performed at three different temperatures using the two surfaces with different roughness. The curves show the cumulative probability of the specific systems having a certain adhesive force. It is seen that for the same temperature, the graph for the 1-micron sample is almost similar to the 240-grit sandpaper sample. The results from the two different experimental studies are in other words a bit conflicting, but it may be explained by the fact that one group used carbon steel while the other used calcite and quartz. The properties of the solid material may therefore play a significant role regarding the adhesion, and aspects like surface free energy, heat capacity and interfacial tension should without doubt be taken into consideration.

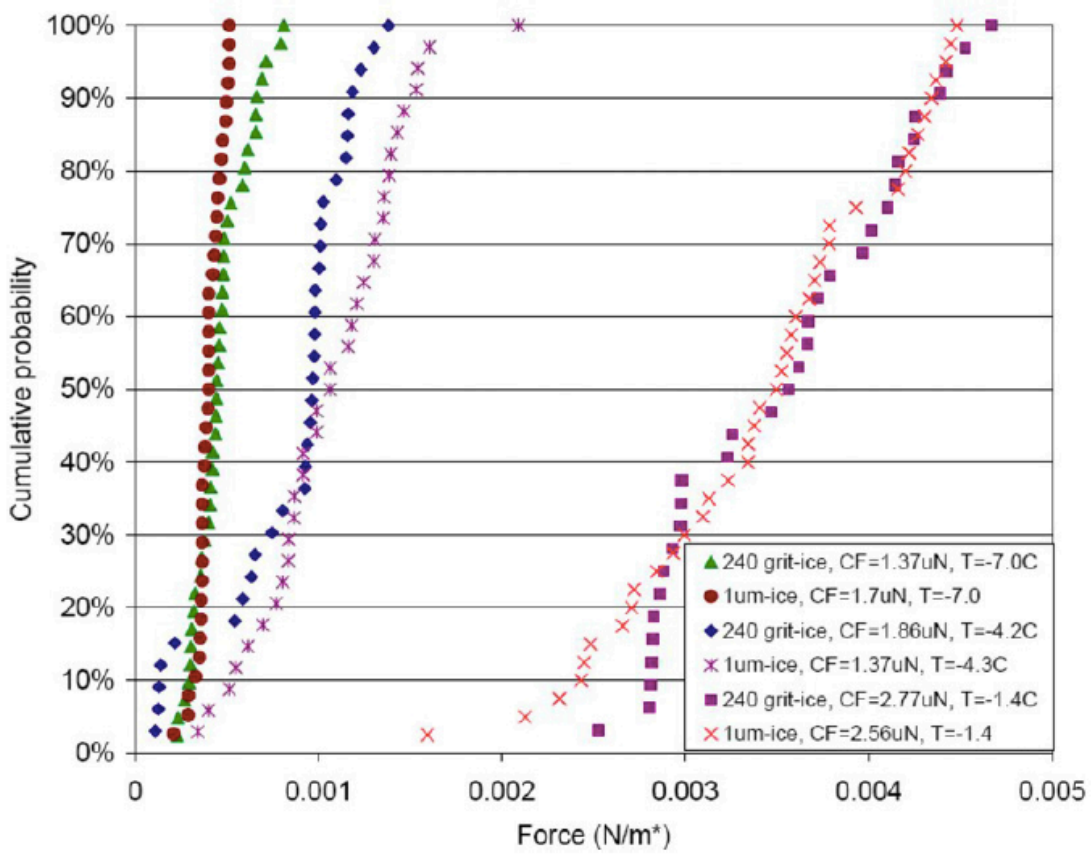

Figure 1.14: Cumulative probability for adhesion force with different temperatures and two different surface roughnesses (Nicholas et al., 2009)

1.10 Liquid Bridging

Liquid bridging is a very important phenomenon when it comes to adhesion and cohesion. The short and simplified version is that a second fluid works as some sort of glue between two similar particles of the fluid in question (Aman, 2012, Ch.4). It may also be between one particle of some substance and a solid surface. As an example, a liquid bridge may be a small portion of water between two particles of hydrate. If this is the case, the presence of water makes the adhesive force increase significantly compared to the force between only two hydrate particles, as explained in the chapter of adhesion and cohesion. This is because the bindings within water are very strong, and water also creates strong bonds with the water molecules in the hydrate.

Liquid bridging involves interaction between three or four different substances as seen in Figure 1.15, and is therefore a relatively complex mechanism. The case of three phases includes two particles of the "main" substance, the liquid bridge and a surrounding phase, where all three are different fluids. Four phases occur when the particle in question adheres to a solid surface with a liquid bridge in-between and a fourth fluid as the surrounding phase.

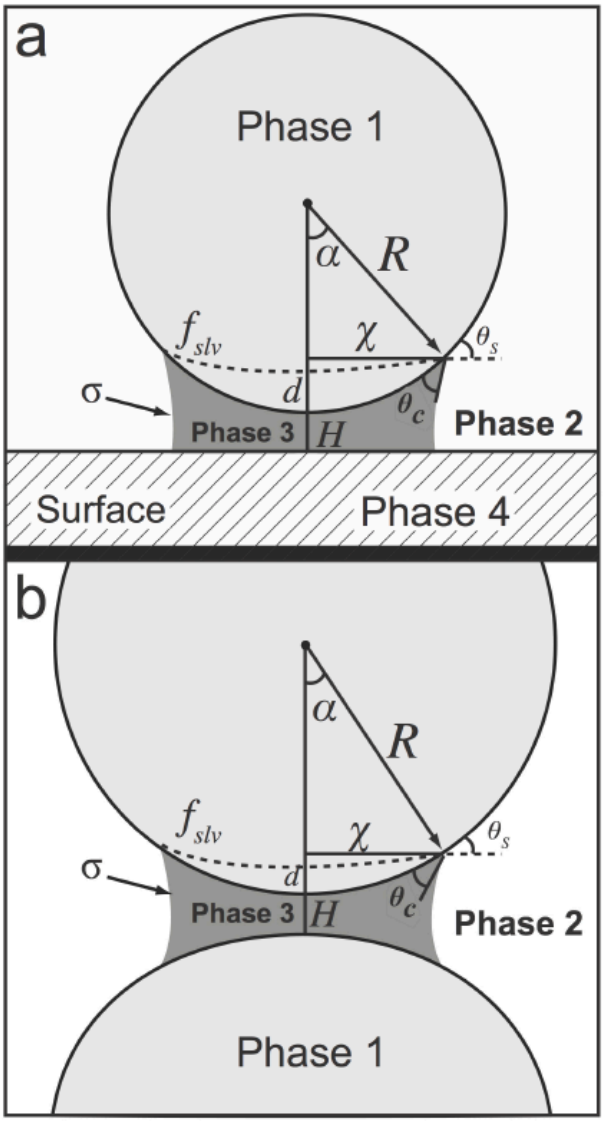

Figure 1.15: Liquid bridging with three (b) and four (a) different phases (Aman, 2012, p.46)

The parameters shown in Figure 1.15 are explained in the following (Aman, 2012, Ch.4). R is the radius of the particle in question. χ is the contact radius if the liquid bridge is cylindrical between the two particles. The contact radius is measured where the liquid bridge is at its widest, this is normally at the interface between the bridging phase and the particle phase. α is the angle created at the center of the particle by one line going through the center of the liquid bridge and the other line pointing to the outermost limit of the liquid bridge. The trigonometric relationship between these three parameters is $\chi = R \cdot \sin\alpha$. f_{slv} is the specific free energy of the contact line between the three phases (solid, liquid, vapor), shown in the figure as the dashed, curved line. d is the immersion depth of the particle in the liquid bridge, i.e. how high up on the particle the liquid bridge reaches. H is the height of the liquid bridge, measured at its center point. σ is the surface tension between phase 2 and phase 3. θ_c is the wetting angle of phase 3 (the liquid bridge) on the surface of the particle. θ_s is the external contact angle of the liquid bridge, occurring between the particle surface and the extended line χ. By using some of the parameters explained above and including a few others, an equation for the cohesive force of the liquid bridge can be derived (Aman, 2012). The equation is given below, where F_A is the cohesive force of the capillary bridge:

$$F_A = \frac{2\pi R^* \gamma \cos\theta_c}{1+\frac{H}{2d}} + 2\pi R^* \gamma \cdot \sin(\alpha) \cdot \sin(\theta_c + \alpha) \tag{3}$$

Here, γ is the interfacial tension between water and oil, and R^* is given by:

$$R^* = 2\frac{R_1 R_2}{R_1 + R_2} \tag{4}$$

R^* is called the harmonic mean radius, and R_1 and R_2 are the radii of the two particles.

Aman (2012, Ch.4.3) highlights the importance of the outer surface layer on the hydrate particles in conjunction with liquid bridging. Experiments have shown that the properties of this surface layer are somewhat different than the rest of the particle, and that these properties indicate that the outer layer are more similar to liquid water than hydrate. This surface is therefore called quasi-liquid layer (QLL), and adds another phase to the system. With the QLL, a liquid-like barrier between the solid particle and the surrounding fluid is defined, making the system more complex. The QLL occurs because some (but not all) of the hydrate melts if the temperature is somewhere around the melting point. If the temperature increases, more of the hydrate particle will melt, leading to an increase of the QLL thickness. Through experiments, it has been found that when the QLL thickness increases, the hydrate cohesive force also increases.

The previously described experiments performed by Aspenes et al. (2009 a, b, c) showed that if water was added to a system of two hydrate particles or a hydrate particle and a solid surface, the adhesive force increased significantly, while acid reduced this force. The main explanation for this is found in the theory of liquid bridging. Water provides a strong bridge between two hydrate particles or one particle and a surface, and this is significantly stronger than if the adhesion is only between the two substances is question. The liquid bridge between a hydrate particle and a solid surface is shown in Figure 1.16.

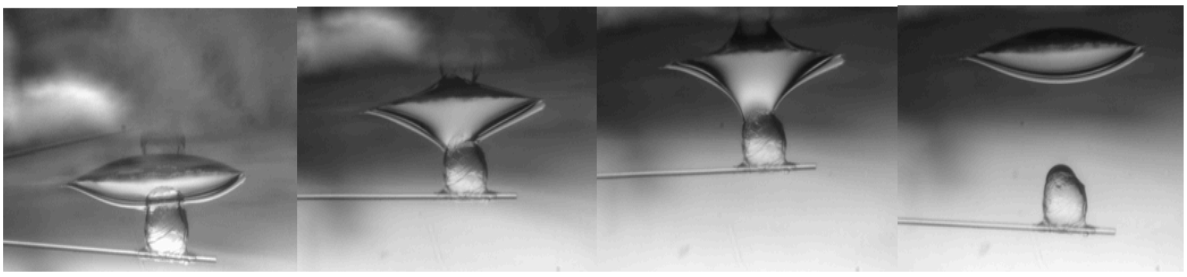

Figure 1.16: Liquid bridge between a water droplet (lens-shaped) deposited on a solid surface and a gas hydrate particle (approximately circular) (Aspenes et al., 2010)

From the figure above, it is seen that the water droplet is stretched relatively far before the hydrate particle is released. This is due to the strong liquid bridge occurring between the two particles in question. With acid on the other hand, the conclusion is quite different. The acid has the ability of changing the wettability of the fluids and solids it comes in contact with, making them more oil-wet. This means that the hydrate particles will be less likely to create strong bonds with liquid water, and the liquid bridges are weaker, if they occur at all. Figure 1.17 shows the same situation as Figure 1.16, i.e. a water droplet on a solid surface and a hydrate particle, but here, the surface of the hydrate particle has adsorbed acids, preventing it from making a strong liquid bridge. It is seen that the water droplet is almost not stretched at all when the hydrate particle is moved away from it.

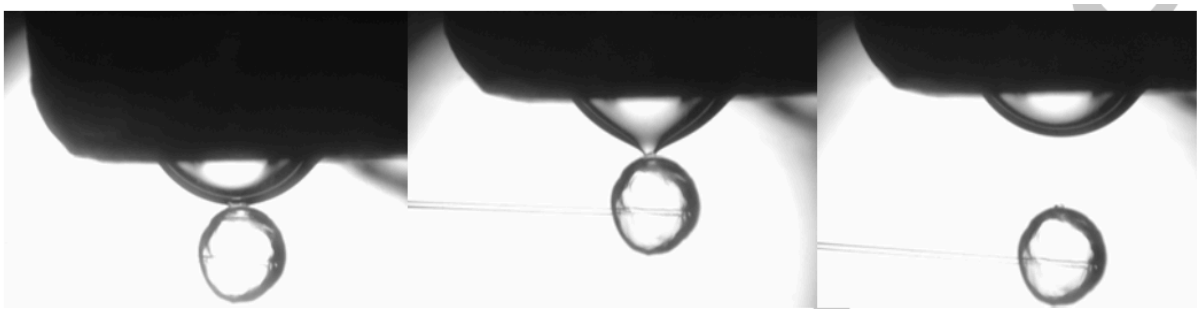

Figure 1.17: Water droplet (top) deposited on a solid surface and a hydrate particle (bottom) with acid adsorption. The liquid bridging between the two particles is very small (Aspenes et al., 2010)

1.11 Hydrophobic & Superhydrophobic Materials

The meaning of the expression hydrophobic is that the properties of a certain material make it repel water to some extent, i.e. water cannot easily react with or affect the material. There may be multiple explanations for this, including interfacial tension between the two substances, different polarity (e.g. that the material in question is non-polar) or simply that the molecules of the material do not "benefit" from reacting with water (sharing of atoms, electrons, etc.) and therefore will try to avoid it. A typical hydrophobic material is oil and this is easy to observe if trying to mix oil and water in a glass. As explained previously in this work, water has a major impact when it comes to adhesion and cohesion between hydrate itself and hydrate and other materials or fluids. Hydrate is therefore obviously not hydrophobic, but adding some hydrophobic material to a system with hydrate and water, the adhesion, growth and agglomeration may change drastically.

Akamine et al. (1992) did experiments to investigate coating on ships and tools that were to be used in arctic conditions (arctic waters). Arctic conditions include low temperatures, ice and often strong wind and large waves in addition to salt water and the other usual sources of wear. This sets high standards and demands to the equipment being used there. The paint or coating on this equipment is usually the only protection between the material it is made of and the surrounding seawater and/ or ice. It is therefore desirable to have a coating that can withstand these extreme conditions and prevent wear on the equipment as good as possible. Akamine et al. defined four important requirements for this type of paint. The first is the resistance against impact – durability – and the property regarding adhesion of the paint to the surface. The second is that the paint should display a small friction and minimal wear in contact with ice. The third requirement involves that the paint repels ice as much as possible, and thus no or very little ice is allowed to adhere to the surface. The fourth is the ability to protect the equipment against corrosion from the seawater. With these requirements, two resin type paints were found as alternatives; epoxy resin and polyurethane resin. The performance of these two resins regarding the requirements mentioned above is shown in Figure 1.18. From this it is seen that polyurethane is much better at impact resistance and drying at low temperatures than epoxy, so Akamine et al chose only polyurethane for further investigation. With the four requirements in mind, it is reason to believe that this type of paint could be beneficial as a coating on the inside of a petroleum production pipe. The paint has proven to be very resistant to wear and corrosion, but most importantly, it makes it very difficult for ice to deposit on it. Since ice has major similarities to hydrate, it is likely that this property also is valid when it comes to hydrate.

Kind / Items	Polyurethan	Epoxy
Impact resistance	◎	△
Adhesion intensity	○	◎
Low friction	◎	◎
Wear resistance	◎	◎
Low ice adhesion strength	◎	○
Corrosion protection (water resistance)	○	◎
Drying property in low temperature	◎	△

(Note) ◎ : Best ○ : Better △ : Good

Figure 1.18: Comparison on the performance of polyurethane resin and epoxy resin regarding the given requirements (Akamine et al., 1992)

The further work done by Akamine et al. on the polyurethane resin was focused on trying to improve the properties mentioned above. The three first of the four requirements were investigated separately, to see which factors were the most prominent for that specific property, and how this could be improved. To improve the impact resistance, it was found

that the mean molecular weight needed to be large, but not too large since that would decrease the hardness of the paint film to an undesirable level. It was also found that OH and NH_2 hardening should be used in combination to avoid foaming. To improve low friction and low ice adhesion, the surface roughness and the ability to repel water was highlighted as important features. It is quite obvious that a high level of smoothness will lead to a low friction coefficient and also low ice adhesion strength. What may not be as apparent is how to get the paint to repel water. The solution Akamine and coworkers found was to add a water-repelling pigment to the composition of the paint, and also use raw materials with low affinity to water and an amine hardening process so that water can not easily absorb into the paint or the paint film. To improve – or more correctly reduce – the ice adhesion strength, it was looked into the possibility of using a primer on the steel equipment before applying the paint in order to increase the bond between the steel and the painting, making it more resistant against any ice that may adhere to the paint film. Through experiments, it was found that a silicon epoxy type zinc-rich primer had very good performance for this specific purpose.

2 Equipment and Experimental Procedure

Figure 2.1: Picture showing the whole equipment setup. The cooler is seen on the right, the pump is on the left, while the pipe with the scraping mechanism is in the middle, submerged in the tank with THF and water

2.1 Liquid Solution

To be able to form hydrate to do experiments on, a hydrate forming fluid was needed. Due to safety aspects, it was desirable to use a hydrate former that can easily form hydrate at atmospheric pressure and at a temperature achievable by the use of a simple cooler. For simplicity, it was also desired that the former was soluble in water. The chemical tetrahydrofuran (THF) has all these properties, and was therefore chosen for these experiments. THF can form hydrate at temperatures below 4.4 °C – which is its hydrate equilibrium temperature (HET) at atmospheric pressure (1 atm). The hydrate formed like this will have structure II, which is by far the most common hydrate structure formed in petroleum production systems. THF is soluble in water and makes a homogeneous mixture that if mixed at the correct proportions can be fully transformed to hydrate. This can be achieved by mixing 21 vol% THF with 79 vol% water, since the stoichiometric ratio between water and THF is 17:1 (Larsen et al., 1997). The mixture then was poured into an open tank made of stainless steel and a volume of about 6 L. The original liquid volume added to the tank was 4.5 L, i.e. 3.55 L of water and 0.95 L THF. Tetrahydrofuran is a solvent that evaporates easily, meaning that the concentration of THF will decrease with time if the tank is left open to the surroundings. It is probably necessary to add more THF to the mixture, but it is very difficult to know if the solution has the desired proportions some time after the very first mixture is made, due to both evaporation and any possible additions. This is however not crucial to know in order to implement the experiment in a good way, the important aspect is just that the solution is capable of forming hydrate on the steel pipe.

2.2 Pipe

The pipe used in the experiments was a steel pipe with an inner diameter of 9 mm and outer diameter of 12 mm, i.e. a wall thickness of 1.5 mm. The pipe is shown in Figure 2.2. The pipe was made of grade 316 stainless steel, which is a type of steel very resistant towards corrosion since it contains molybdenum (AK Steel, 2016). The molybdenum makes it more protected against fluids consisting of acids like sulfate, hydrochloride, acetate and alkaline chlorides. Grade 316 steel is relatively "soft" steel that can easily be shaped and bent without creating stresses in it or otherwise changing the properties of it significantly. The pipe used in these experiments first started out as a straight pipe, being cut and bent to the desired shape and size. It was initially made into a U-shaped equipment with two 90° bends and three equally long sections of 20 cm each. Later, it was found that the one upward facing section needed to be shorter for an easier practical implementation of the experiment, and therefor it was cut. The "bottom" part of the pipe was then placed in two small holders, giving it a small, flat surface easy to attach to a second flat surface. The holders were welded to a round, heavy flange, giving it a good stability towards any vertical pressure or stress the pipe may be exposed to, seen in Figure 2.5.

Figure 2.2: The steel pipe with high roughness. The section to the right is where the scraping was conducted

After several experiments had been conducted with the pipe described above, the pipe was changed to another with some other properties. This was also a grade 316 stainless steel pipe with an outer diameter of 12 mm, but the inner diameter was 10 mm (wall thickness of 1 mm) and the surface of the steel had a lower roughness than the first pipe, making it smoother. This was done in order to see how large influence the surface roughness has on the strength of a hydrate deposit, and also if the roughness affects how easily a deposit occurs on the surface. Unfortunately, there are no measurements on the exact roughness of the pipes.

2.3 Cooler

The cooler was used to decrease the temperature of the pipe in order to create hydrate-forming conditions in the system. The cooler was a refrigerated/ heating circulator called FP50 – MH from the manufacturer Julabo. The main parts of the cooler are a tank filled with a mixture ("cooling bath") of water and glycol, with a coil submerged in it. The tank has two openings on its side where hoses can be attached, one for fluid going out of the cooler and one for the returning fluid. The coil uses electrical power to cool the fluid in the tank to a temperature determined by the user, before the fluid flows in a loop through the two hoses and any equipment that the user wants to cool. In the case of these experiments, the two hoses were attached to the two ends of the steel pipe, making the cooling fluid flow through it. The mixing proportions of water and glycol is unknown, but at the start-up of the experimental period it was necessary to add more glycol to the cooling bath in order to get the temperature down to the desired level. It is important to note that any leakage from the cooler hoses connected to the pipe should by all means be avoided, as glycol would work as an inhibitor in the THF solution and slow down or avoid hydrate formation (Sloan & Koh, 2008, p.644).

2.4 Scraping Mechanism

The tools used to scrape the hydrate from the pipe were partially specifically made for these experiments. It consisted of three main parts; a pump, a piston and a tailor-made scraper. Each of these is shown below. The pump was a simple hand pump with oil as the pumping fluid and a handle used manually to increase the pressure. The hose from the pump was connected to a piston that increased in length when the pressure increased, meaning that it pushed the scraper connected to it downwards. The tailor-made scraper was made of a cylindrical object of steel. The subject was initially a compact cylinder, but was hollowed into a pipe-like section, consisting of two different inner diameters. A small part of the cylinder had a diameter of just above 12 mm to fit around the steel pipe, while the rest had an inner diameter of 18 mm to attach it to the piston and also to be able to connect the hose from the cooler to the steel pipe. This was made possible by making a slit in the cylinder. The tip of the cylinder facing downward to the steel pipe was shaped conical in order to scrape the deposits made on the pipe.

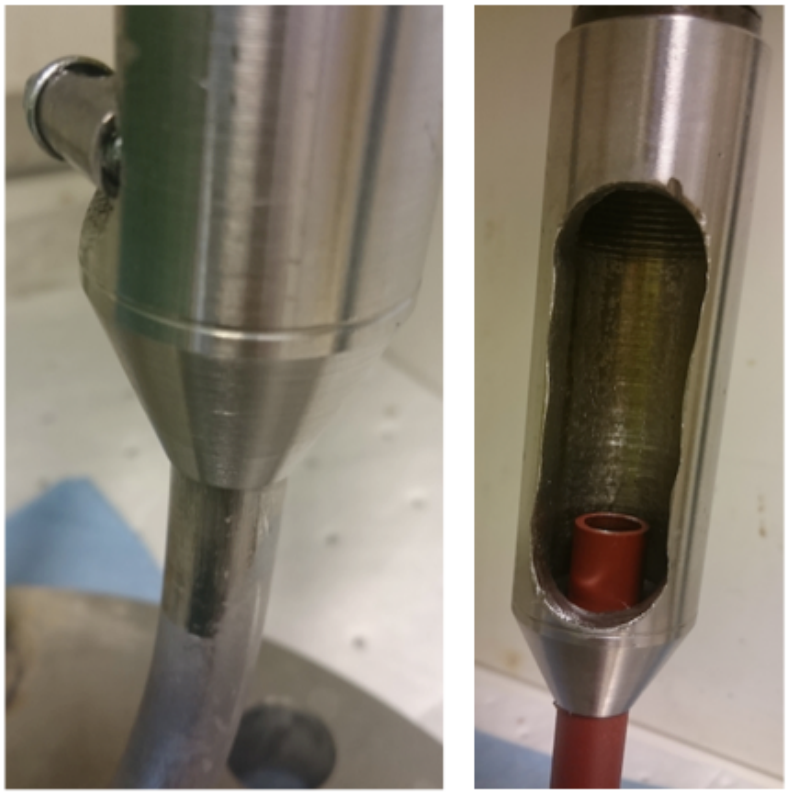

Figure 2.3: Pictures showing the cylinder for scraping. To the left is a close-up of the angled section of the cylinder and the pipe inside. The picture to the right shows the slit made to attach the pipe (red) to the cooler hose (not shown)

Figure 2.4: The pump (left picture) used to provide pressure to the piston (right picture). The picture to the right also shows the two rods used as holders for the piston/ scraper mechanism (seen at the bottom) and the manometer seen in the upper left corner

2.5 Equipment Setup

The full equipment setup can be seen in Figure 2.1. More detailed pictures are seen in Figure 2.5 and Figure 2.6 below. Figure 2.5 is from when the smooth pipe had been coated with a primer, while Figure 2.6 is from the experiments with the pipe with high roughness without coating. The steel pipe was as mentioned attached to a round, flat flange by using two holders welded to it. Two long rods were also attached to the flange in order to make a rack for the pumping/ scraping mechanism. A steel plate with holes for the rods was placed between them, providing a flat surface where the piston and scraper could be hung from. A small section of the steel pipe then was put inside the cylindrical scraper, before one of the hoses from the cooler was attached to the pipe through the slit. The other hose was connected to the other end of the pipe. The hand pump then was attached to the piston, but with a manometer between the two parts in order to measure the pressure being transferred from the pump to the piston and scraper. The flange and everything attached directly to it (the pipe and the piston/ scraper) was then put in the steel tank, and the liquids to be used for the experiment were poured into the tank. All of the equipment except for the cooler was placed inside a small compartment with an exhaust fan due to the possible harmful gasses occurring when tetrahydrofuran evaporates.

Figure 2.5: Picture showing the steel pipe attached to the flange with holders and to the scraping mechanism. The yellow hoses are connecting the pipe and the cooler, while the black hose to the left is connecting the pump to the piston. The manometer is at the top

Figure 2.6: Picture showing the pipe submerged in the tank filled with THF and water. The scraper is seen to the right between the two rods

After several experiments had been conducted, it was observed that some of the horizontal section was getting bent due to the large force applied to the vertical section. To compensate for this, a flat, 1 cm thick slice of steel was placed between the pipe and the flange it was attached to. This is shown in Figure 2.7**.** The slice completely filled the open space between the pipe and flange, avoiding additional bending of the pipe. A fortunate side effect of installing this piece was that the piston got pushed back up to its starting position by itself instead of doing it manually by hand. This was because there was no opening between the pipe, the steel slice and the flange, so when the vertical section of the pipe was pushed slightly downwards due to the piston, a small pressure between the three parts occurred. When the pump pressure was removed, this pressure was also released, causing the piston to be pushed back up.

Figure 2.7: A slice of steel was placed between the steel pipe and the flange to avoid bending of the pipe

2.6 Coatings

Two different coatings were tested in these experiments. Each coating was contained in a spray can – seen in Figure 2.8, i.e. they were sprayed onto the surface of the pipe. One coating was automotive paint made of acrylic, while the other was a type of primer used to hinder corrosion. The main ingredients in this second coating are 2-butanone oxime and zirconium. Since two different pipes were used in the experiments, they got sprayed with one coating each. The pipes originally had some different properties, mainly regarding the roughness, so this may have had an impact on the result after coating was applied. The pipes were cleaned with soap and water to remove both the hydrate former and any impurities at the outer surface and glycol solution from the inside of the pipe. Then they were dried thoroughly before the coating was applied. The desired results when applying the coatings was a thin, evenly distributed layer around the whole outer surface of the pipes. This was well achieved with the primer, but was more challenging with the acrylic spray. The acrylic spray was thicker than the primer, and some of it began to trickle down the pipe when the layer was not thin enough. It was also difficult to get an even layer at the whole surface as the spray somewhere both accumulated and separated, making an uneven pattern at the surface. The most important section of the pipe, i.e. where the scraping was conducted, did however get a reasonably thin and even layer. This makes it valid to assume that the surface of the acrylic paint has a higher roughness than the primer, although the acrylic paint visually had a more slick and shiny appearance.

Figure 2.8: The two coatings tested in the experiments. Automotive paint on the left and corrosion-avoiding primer on the right

Another challenge appeared when the pipes were put in place in the other equipment. From the previous experiments the pipe with the highest roughness had gotten a bit bent, so it was difficult to place it correct in relation to the scraper. Because of this, some of the coating was removed from the surface by the scraper already during the installation of the pipe. This is obviously a large source of error regarding the results, as the coating was only partially covering the surface in question. Some of the coating from both pipes also got removed

during the experiments due to the scraping procedure and the other forces it experienced (cooling, heating, hydrate formation and dissolving). The pipes with the different coatings are shown in Figure 2.9 below, both before and after the experiments had been completed.

Figure 2.9: The pipe with high roughness coated with automotive paint (left) and the smoother pipe coated with corrosion-avoiding primer (right). The left pictures of each coating are before the experiments, the right ones are after

2.7 Procedure

The experiments were done in a cycle that was repeated several times to get a certain quantity of comparable results. Each cycle started with setting a temperature on the cooler. This temperature is the one that the cooling fluid would have when leaving the cooler through the hose. The fluid flows through the hose, then the steel pipe over to the return hose before it's back inside the cooler. The cooler fluid is likely to have a higher temperature when returning to the cooler due to heating from the hose, pipe and surroundings. If the cooler is left at the preset temperature for a while after this temperature is reached, the temperature difference between the fluid going out of the cooler and the fluid returning to it would be relatively small. It is however important to note that the temperature being set at the cooler will not be achieved at the outer surface of the steel pipe due to the heat capacity of the steel and heating from the surroundings. For the steel pipe to be able to reach this temperature, all of the surrounding fluid in the tank would need to be cooled to this temperature, demanding a significant amount of time and energy, being very inconvenient for the implementation of the experiment. Due to this, it was found early in the testing of the experimental procedure that the temperature set for the cooler needed to be somewhat lower than what was initially planned. Theoretically speaking, hydrate would be formed with a temperature below 4.4 °C when using THF, but the setting temperature for the cooler was required to be – 4 °C before hydrate was initiated.

For both the experiments with ice and with hydrate, two different temperatures were used. For ice, – 4 °C and – 5 °C were used. However, for the experiments with – 4 °C, the cooler temperature was first set to – 5 °C to provoke the formation of ice before it was set to – 4 °C. In these cases, the cooler was only held at – 5 °C for a short time before the setting

temperature was changed to – 4 °C. The reason for this procedure was that without cooling down to – 5 °C first, very little ice was formed, and it also took longer time. This was also done for some of the hydrate experiments with – 5 °C. In these cases, the temperature was set to – 7 or – 8 °C until hydrate formation occurred, before it was raised to – 5 °C for the no-touch time. For the experiments with hydrate, – 5 °C and – 10 °C were used as the testing temperatures. The relatively large difference between the two temperatures was chosen to see the influence of the temperature on hydrate formation, thickness of the layer and most importantly the strength of the deposit.

After the cooler temperature was set, it took a couple of minutes before this temperature was reached. When it was reached, the system was left to stabilize for a pre-determined amount of time. This time was changed during the experiments, reaching from 1 (usually 2) minutes up to 15 to see the impact of this "no-touch time" (NTT). All the different NTTs were tested several times to get a comparable amount of results. When the NTT of the specific experiment had passed, the main part of the whole experiment was performed; the scraping. First, it was assured that the pump was set in the closed position and that the pressure gauge was reset from the previous measurement. Then the pressure was increased manually using the pump. The piston slowly pushed the scraper tool downward toward the interface of the liquid as the pressure increased. The pressure was increased until the upmost deposit formed right below the interface had been scraped off of the pipe. Right before the scraper tool reached this point, the pressure would increase rapidly before the scraper "slipped" through the ice/ hydrate and the pressure decreased. The peak pressure (P_{max}) in this procedure is the targeted value in these experiments. After this value was found in the specific experiment, a valve in the pump was opened in order to let the oil from it flow back and by this reduce the overpressure back to zero. In the case of experiments with ice, the cooler temperature was set to 2 °C in order to melt the ice before the next experiment. Hydrate requires a higher temperature to melt, so in these cases, the temperature was set to 4.5 °C after the scraping procedure was performed. After the melting, the scraper tool needed to be pushed back up in the starting position, the valve on the pump was closed again, the bottom part of the scraper was dried with a paper towel to remove any liquid and the manometer was reset. These steps represent the end of an experimental cycle, meaning that when they had been completed, a new cycle could be initiated.

3 Results

3.1 Hydrate Formation

When using tetrahydrofuran, hydrate should theoretically be formed when the temperature drops below 4.4 °C. But as explained earlier, it was found that this boundary could not be used for the cooler temperature in the experiments. A cooler temperature of at least – 4 °C, and preferably – 5 °C and below, was needed before the hydrate formation occurred to a significant extent. Therefore, the two temperatures – 5 °C and – 10 °C were used in the experiments with hydrate. It was seen that hydrate was usually, but not always, formed relatively spontaneously when the cooler temperature had reached – 5 °C. In the cases where hydrate was not formed at once, stirring a bit in the tank fluid often had a desirable and quick effect. This phenomenon is due to the fact that once a system is inside the hydrate forming region, the system may or may not form hydrate immediately and it is somewhat unstable as long as hydrate has not yet been made (Sloan & Koh, 2008). When this is the case, only a small movement or force applied to the system can trigger it to initiate hydrate formation. However, the movements and stirring in the tank liquid was not always enough to trigger the hydrate formation. In these cases the temperature was lowered down to – 7 or – 8 °C for a short period of time before it was raised back up to – 5 °C and the no-touch time was started. This challenge was most prevalent late in the experimental period. Figure 3.1 shows some pictures of the hydrate formed through the experiments.

Figure 3.1: Hydrate deposit on the steel pipe (left) and after removal from the pipe (right). The upper right picture shows the hydrate while floating in the tank fluid, in the lower picture it is placed on a dry surface at room temperature

3.2 Temperature Dependence

For the experiments with ice, two temperatures were tested, and the difference between them was only 1 °C. Since the temperature difference was so small, the pressure readings between these experiments were expected to be relatively similar, although a bit lower for the higher temperature. The plots from all of the experiments for both temperatures are seen below. Here, the pressure is plotted as a function of the no-touch time. It is seen that the overall trend is that the pressure is in fact a bit lower for the experiments with – 4 °C than the ones with – 5 °C. The high pressure readings for 1 minute no-touch time for the – 5 °C experiments is due to very little formation of ice in these experiments, and the equipment was also a bit misaligned, so these results should not be given a lot of attention. This is also the case for some of the high readings at 2 minutes NTT at the same temperature. If these results are neglected, it is seen that the average pressure for the three longest NTTs is fairly close to each other, between 12 and 17 bar. In the experiments with – 4 °C, the pressure readings for the shortest no-touch time are very low. These results are more trustworthy than the ones from the experiments with – 5 °C and short NTTs, but one should however take one point into consideration. Just before these experiments were done, some of the equipment was adjusted a bit due to a large misalignment between the pipe and the scraper, and these parts were fitted better relative to each other. This may have resulted in lower pressure readings than in the other experiments, so the relative difference between NTT = 2 min and the others with higher NTT is possibly lower than the graph shows.

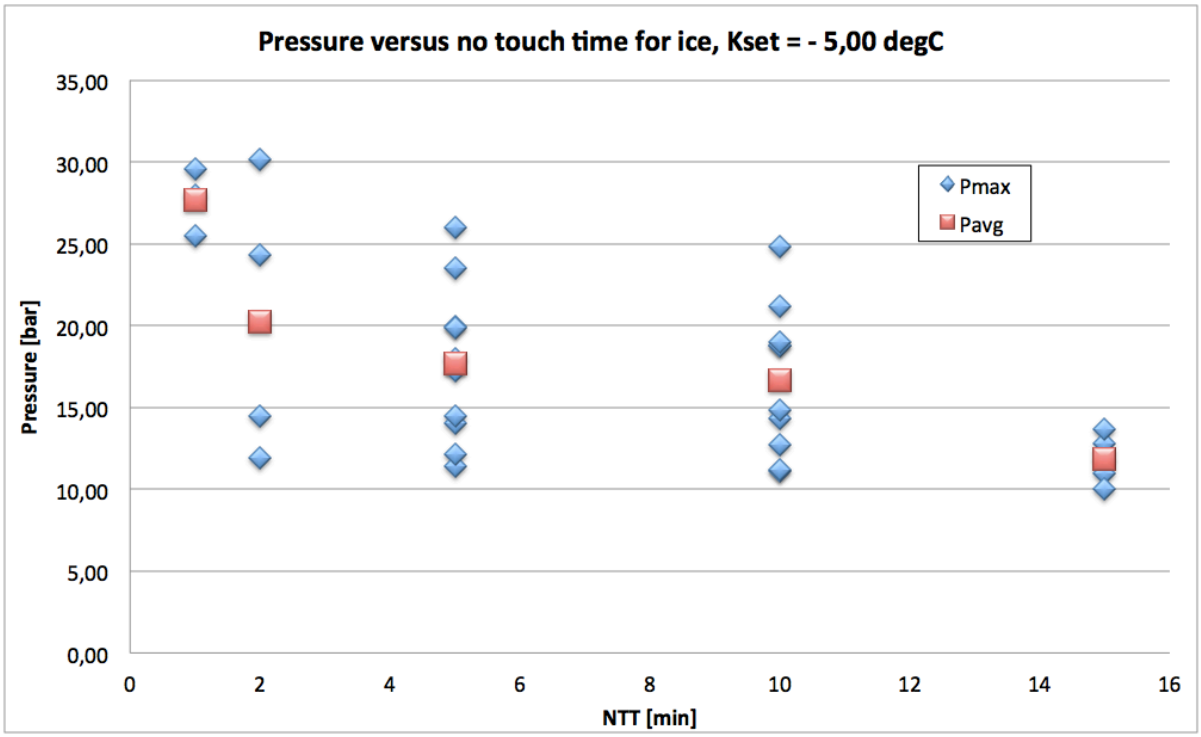

Figure 3.2: Strength of ice deposit on a steel pipe, cooler temperature is – 5 °C

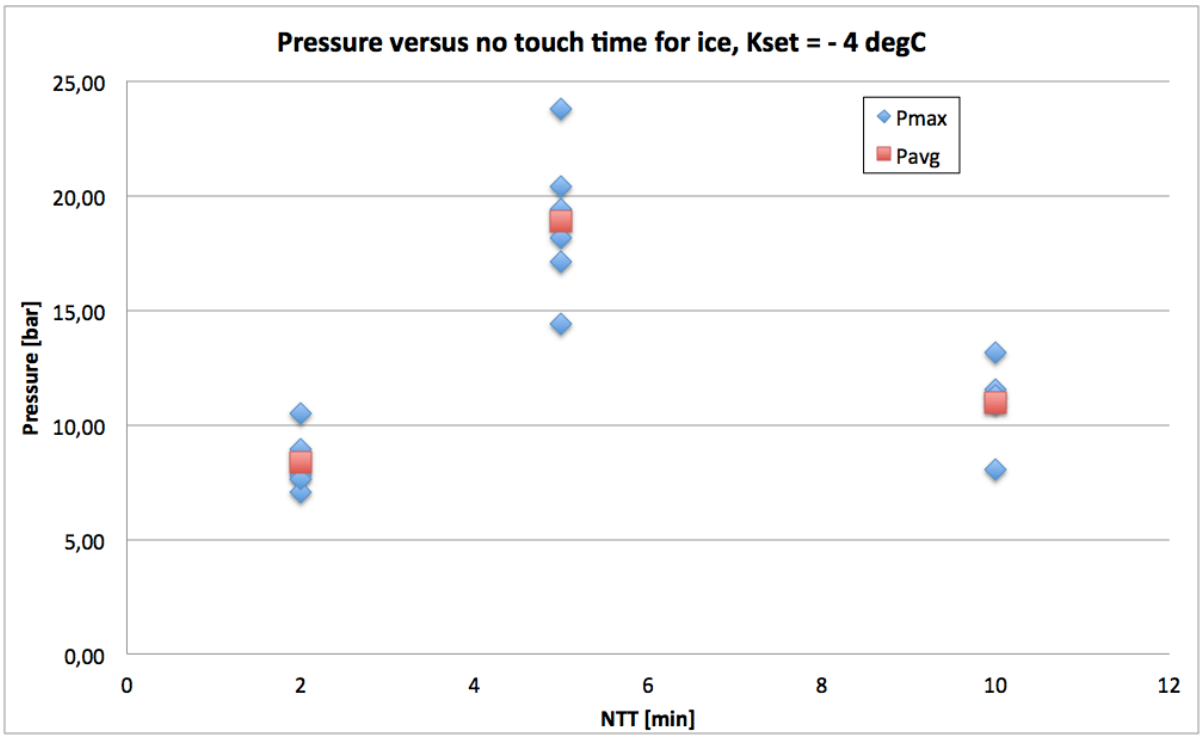

Figure 3.3: Strength of ice deposit on a steel pipe, cooler temperature is – 4 °C

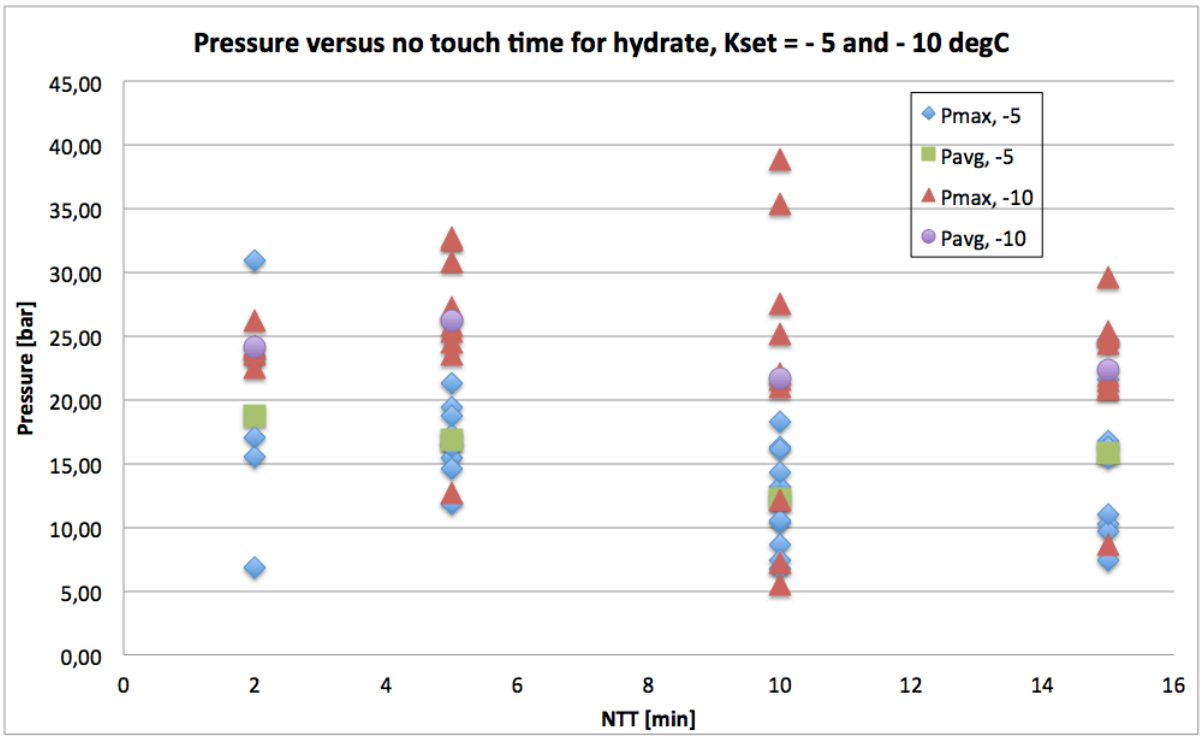

Figure 3.4: Pressure versus no-touch time for the base case for both the tested temperatures

For the experiments with hydrate, the difference between the testing temperatures were larger, hence the pressure difference was expected to be larger. Hydrate formation was initiated at a cooler temperature of about – 5 °C, so this was one testing temperature, while the other was as low as – 10 °C. Not surprisingly, the lowest temperature led to a higher degree of hydrate formation, i.e. the deposit layers were thicker. As can be seen in the graph in Figure 3.4, the

pressure readings for the – 10 °C experiments are higher than the – 5 °C ones. The average pressures for the experiments at – 5 °C is between 12 and 18 bar, while the corresponding numbers for the – 10 °C experiments lies between 21 and 26 bar. The results are from the base case experiments (the pipe with high roughness).

The temperature of the experiments also had an impact on the thickness of the deposit layer, i.e. a lower temperature results in a thicker layer. This is clearly shown in Figure 3.5 below. Only three of the values from the experiments with – 10 °C is within the same range of thickness as the results from the experiments with – 5 °C, while the rest has higher thicknesses. The graph also gives a clear indication that higher thickness leads to higher pressure, i.e. increased adhesive strength of the deposit. The two trend lines and their equations included in the plot are relatively similar, indicating that this relationship may be close to proportional.

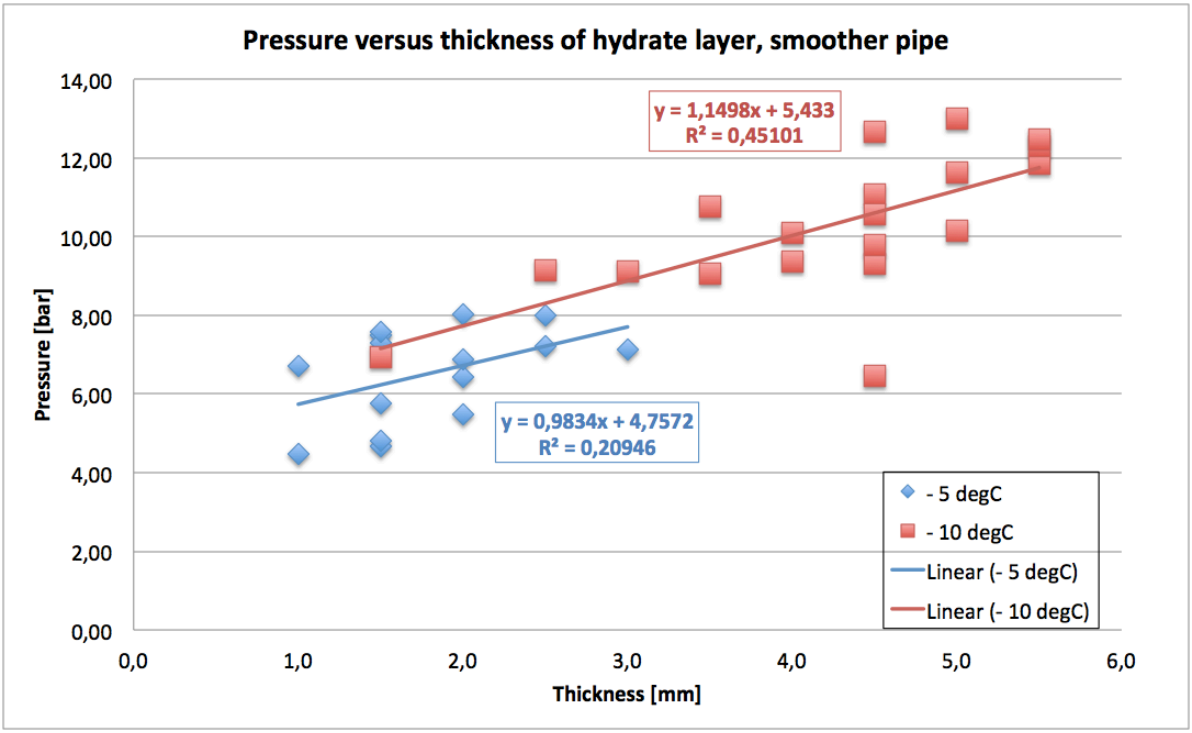

Figure 3.5: Relationship between thickness of hydrate layer and the pressure needed to remove it for both - 5 and - 10 °C. The results are from the experiments with the smooth pipe. Trend lines with equations and the fit of these (R^2) for both temperatures are included

3.3 Strength of Hydrate Deposits

The figure below shows the average pressure values for each tested no-touch time for all of the different experiments. This includes all the tested temperatures, both the rough and smooth pipe and the two coatings. The average values include *all* experimental data. Hence some of the data points in the calculation have significant errors associated with them, but the average values can be trusted to be relatively accurate. It is seen from the plot that all of the average values for the experiments with hydrate at – 10 °C with the rough pipe are the highest ones, while the hydrate experiments at – 5 °C with the smooth pipe and the experiments with the smooth pipe coated with primer have the lowest average values. These average values have a large span, with the lowest at about 5 bar, while the highest is as much as 27 bar. This clearly shows that the different parameters tested in the experiments have an impact on the adhesive strength of the deposits. These will be discussed in further detail in chapter 4.

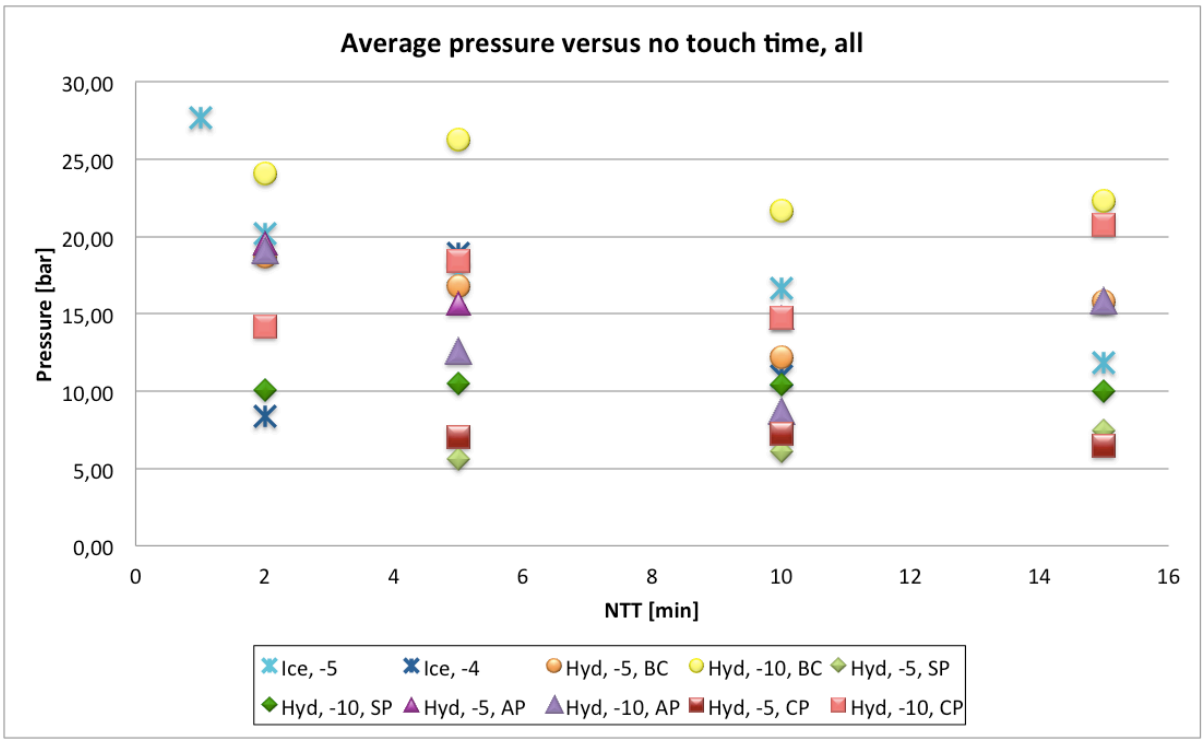

Figure 3.6: Plot showing the average pressure for the different no-touch times for all the cases. BC = base case, SP = smoother pipe, AP = automotive paint and CP = corrosion-avoiding primer

Different no-touch times were used in the experiments, and Figure 3.7 shows an example of results where pressure is plotted against the deposit thickness and the different NTTs are seen. The example is from the case with the smooth pipe. As can be seen from the points and the included trend lines, there are no significant difference between the three no-touch times, regarding both the pressure and the thickness of the layer. The plot does however show a clear relationship between the thickness and the pressure.

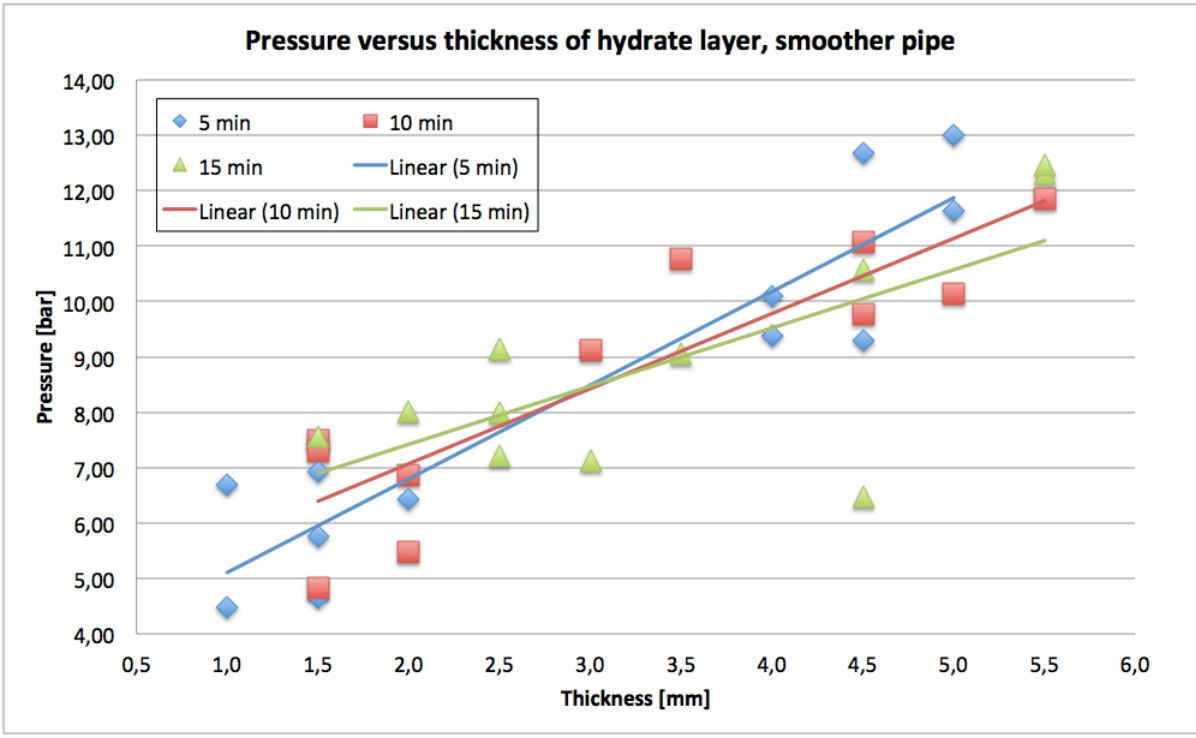

Figure 3.7: Plot of pressure versus thickness where the different no-touch times are seen

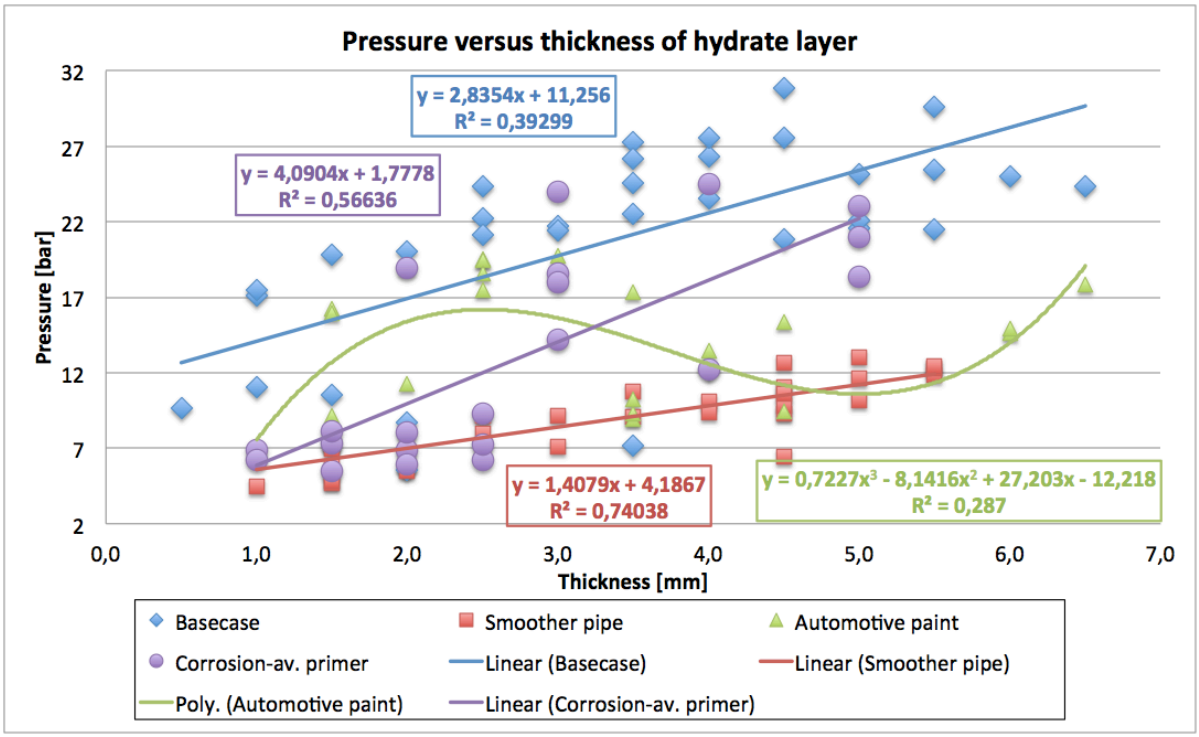

Figure 3.8: Pressure versus thickness for all the different hydrate cases

The thickness of the hydrate deposit formed in each experiment was measured in many, but not all of the experiments. A plot showing all the experiments where thickness was measured for all the cases with hydrate is seen in Figure 3.8. A trend line is added for each case, and the equations for these and how well they fit are shown in the plot. All the trend lines except one are linear lines, giving a fairly good fit to the data points. The trend line for the case with automotive paint is a third degree polynomial line, since a linear line was a very poor fit. The

data points from this case is in the intermediate to upper level for the experiments with low thickness, but for higher thicknesses the pressure readings decrease to the lower level.

All of the given results from the experiments are given in the unit of bar, since this was the readout from the manometer connected to the equipment. This means that the values show the *pressure* needed to remove the deposit from the steel pipe. A parameter that may be at least as interesting as this, is the *force* needed to do the same. The force F [N] is found by multiplying the pressure P [bar] with the surface area A [m^2], i.e.

$$F = PA \tag{5}$$

where the surface area is found by multiplying the circumference of the pipe by the height. The challenge is however how to define the height. The pressure found in the experiments is the maximum pressure occurring when the deposit breaks off of the pipe. This means that the logical height to use in the calculations is the length of the deposit that breaks off. But this length has not been measured in the experiments, and it is very likely that this parameter had a significant span in the values from the different experiments. An approximation for this length is somewhere between 0.3 cm and 1.1 cm, but in most cases it is believed to be around 0.5 cm. The table below shows the impact the inaccuracy of this number gives. The pressure-values used in the table are some randomly picked numbers from the whole span of the experimental results. The values from 0,003 to 0,011 are the height, given in meters.

Pressure converted to force						
Diameter	0,012	m				
Circumference	0,038	m				
Pressure [bar]	**Pressure [Pa]**	**Force [N]**				
		0,003	**0,005**	**0,007**	**0,009**	**0,011**
5	500 000	57	94	132	170	207
10	1 000 000	113	188	264	339	415
15	1 500 000	170	283	396	509	622
20	2 000 000	226	377	528	679	829
25	2 500 000	283	471	660	848	1 037
30	3 000 000	339	565	792	1 018	1 244

Table 3.1: Pressure needed to remove the hydrate deposit, converted to the corresponding force. The bold values below "Force [N]" represent the possible heights of the deposit removed

The table shows a large difference in the force values for the different values for the height. The highest assumption for the height is almost four times higher than the lowest assumption, resulting in a force that is almost four times higher. If the span of the height is narrowed down to 0,5 cm and the two values above and below it, the difference is smaller, but the highest value is still more than two times higher than the lowest, since the assumption for the height is also more than two times higher. The value of the height is therefore an important parameter in calculating the force, so this needs to be measured more accurately to get a more trustworthy result. If the parameter is defined to be exactly 0.5 cm, it is seen that the force needed to remove a deposit of ice or hydrate is between 100 and 600 Newton.

3.4 Impact of Coatings

The two coatings tested in the experiments were sprayed onto two different pipes with different surface roughness. The automotive paint gave a more uneven and a bit thicker layer than the primer, which gave an additional difference in the assumptions for the cases. Figure 2.9 shows that a significant amount of the coatings were torn off from the pipe during the experiments, so the results are not completely accurate. The plots for pressure versus no-touch time are shown below. A clear difference between – 5 °C and – 10 °C is seen for the primer experiments, with the lowest temperature having the highest pressure readings. For the automotive paint case, the trend is rather surprisingly the opposite, with higher pressure readings for the low temperature. The logical explanation for this is that the experiments with – 10 °C was completed first, and then the – 5 °C ones. This means that the experiments with the low temperature was done when all or most of the coating was still intact, while a lot of it had been removed when the warmer experiments were conducted. This problem also occurred for the primer case, but at a later point in the experiments so only a few experiments were affected. The average pressure for the automotive paint case at – 5 °C is between 14 and 20 bar, while it has a larger span for the – 10 °C experiments, ranging all the way from 8 to 19 bar. For the experiments with corrosion-avoiding primer, the average pressure values is almost equal for all the experiments at – 5 °C, being around 7 bar. At – 10 °C, the corresponding values lies between 14 and 21 bar, i.e. two to three times higher.

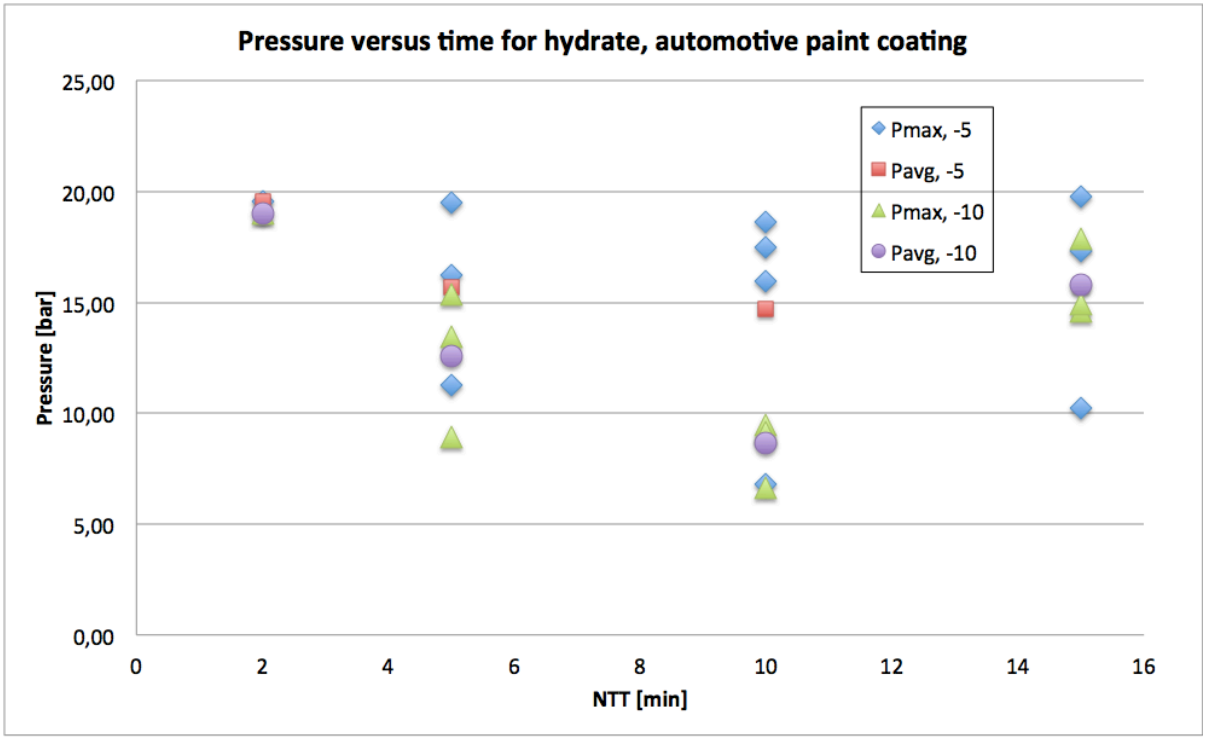

Figure 3.9: Pressure needed to remove hydrate deposit, plotted against the no-touch time for the case with automotive paint as the coating

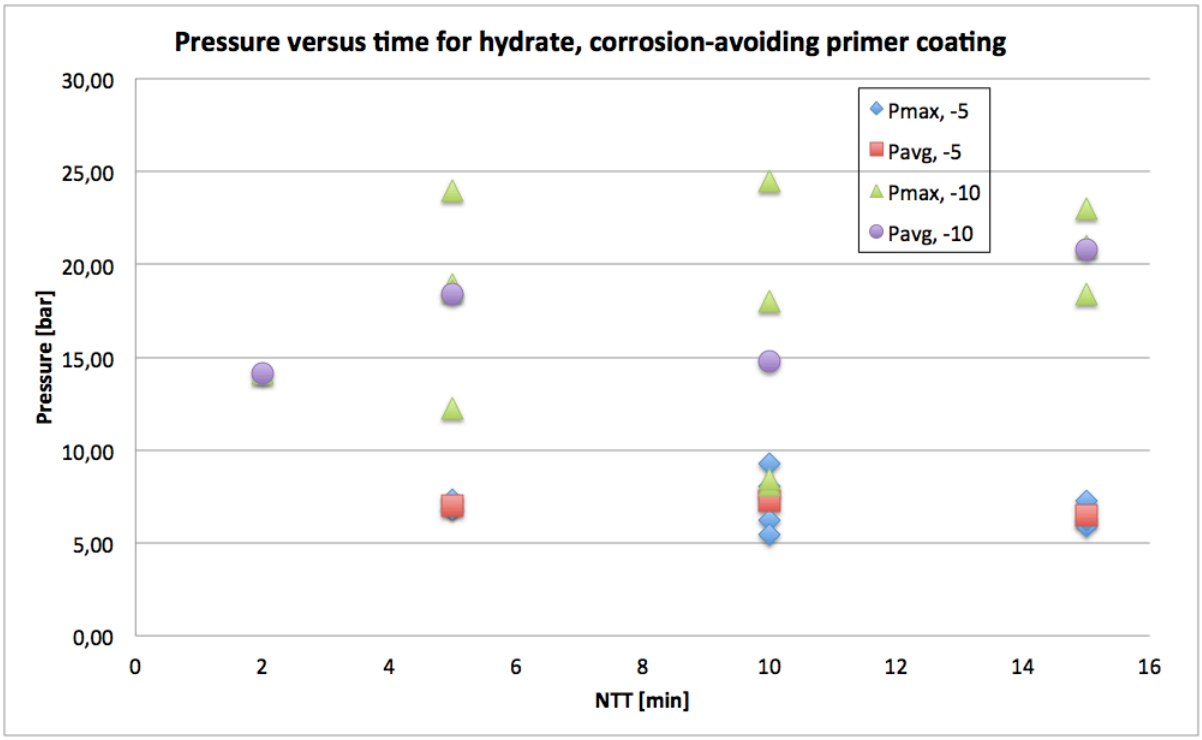

Figure 3.10: Pressure needed to remove hydrate deposit, plotted against the no-touch time for the case with corrosion-avoiding primer as the coating

4 Discussion

4.1 Implementation of the Experiment

Much of the equipment used in these experiments was made specifically for this, and it may be difficult to do the exact same experiment at a later time. But the principle that is tested is more universal, and can be verified and tested again in different experiments. The most important aspects is to have some sort of a solid surface, a substance that forms hydrate at the surface, tools to remove this and measure the pressure/ force needed to do so, and possibly a system to adjust the conditions into the hydrate formation zone, like a cooler or a pressure chamber. Since no similar experiment like this had been done before the start-up, it was unclear what equipment was the best fit for it, and how to solve the different challenges. As an example, it was found that the pipe got bent by the pressure from the piston after several experiments were completed, so adjustments of the equipment were made during the experimental period. The best procedure for the experiments was also found after numerous attempts. With that being said, it should be mentioned that almost all of the experiments were executed in a sufficiently good manner, and gave a useful result for the desired parameters of the work.

Before the experiments were started, it was believed that hydrate would be formed at 4.4 °C, since this is the hydrate equilibrium temperature for tetrahydrofuran. This value could however not be used for the temperature of the cooler, due to heat capacity and heating from the surroundings. The temperature of the cooler needed to be at least – 5 °C for hydrate formation to take place. At this temperature, hydrate was formed at a sufficient rate to be able to do the measurements, although the system sometimes needed to be triggered to start the formation. As seen in several of the figures above, for example Figure 3.4 and Figure 3.5, the experiments with the lowest temperatures gave the highest pressure readings. A visual observation of this was that at – 5 °C, the hydrate was often a bit "soft" and it simply just slipped off the pipe, while at – 10 °C, the hydrate was more brittle and it broke off the pipe with a significant notch of the scraper. This means that the temperature has a large impact on the properties of the hydrate, and the colder it gets, the more difficult it is to remove.

One concern before the start-up of the experiments was whether or not the scraper would remove the hydrate at the interface between the hydrate and the pipe, or just the outer layer of the hydrate and leave the inner layer due to the small gap between scraper and pipe. During the experiments, a visual observation of this was that the scraper did in fact remove all of the hydrate deposit, but the observation is not completely reliable. There could have been a very thin layer left, being difficult to detect. However, based on the results, it seems as if this was not the case. If the scraper had only removed the outer layer, all of the results would be much more similar since the measurements would only be of the hydrate *cohesive* strength, and the pipe surface would have no impact. But the results show significant differences between the cases, and hence it is safe to believe that the measurements are of the *adhesive* strength between the hydrate and the solid surface.

4.2 Sources of Error

The experiments done for this thesis have several sources of errors connected to them. Some are likely to be close to negligible regarding the main focus of the work, while others may have a significant impact on the results. The possibly largest and most important source of error is several cases on inaccuracy. As an example, the no-touch time only had an accuracy of ± 2 minutes. The timer was sometimes started a bit before or after the preset cooler temperature was reached, and the scraping procedure was not always implemented exactly at the point the no-touch time was reached. In several cases where the timer was started a bit too "late", the reason was that the hydrate formation had not started yet, and therefore the timer was not started until the formation occurred. This inaccuracy is likely to have caused a difference in the deposit thickness even when all other parameters were identical. Another case of inaccuracy was the measuring of the deposit thickness. The measurement was made at the opposite side of the pipe from where the scraping was done, and hence it cannot be used directly to show any possible proportionality between layer thickness and the adhesive strength of this. A simple caliper was used for this, and the readout of this only had an accuracy of about ± 1 mm. It should however be noted that the measurement was made at approximately the same location every time, so the different results can be compared to each other.

A third source of inaccuracy is one that may be of larger importance than the others, namely *where* the maximum pressure is measured. The desired location to measure is right at the interface between liquid and air, i.e. at the upper boundary of the deposit on the pipe. In some experiments, it was observed that the ice or hydrate was compressed a bit before it broke off the pipe, and other times it didn't "break" off at all, it was just simply removed without any clear "notch" in the pressure build-up. In these cases, the maximum pressure readout from the pressure gauge is likely to come from a different location on the pipe than in the other experiments. There also exists (at least) two other sources of inaccuracy regarding the scraping mechanism, and both of these are connected to the physical equipment setup. The top of the steel pipe was as mentioned placed inside the bottom part of the scraper. It was a little challenging to adjust these two parts into a perfectly leveled fit, so it is likely that there was some angle and skewness between them. This would have led to the pipe being in direct contact with the scraper at one side, and therefore the scraper has been required to move down the pipe, and not just the hydrate deposit, possibly increasing the friction and hence pressure significantly. It was observed that this in fact did happen in several of the first experiments, giving very high pressure reading, and it also made it difficult to manually push the scraper back to its starting position after an experiments was done. It actually happened to such a large extent that some of the surface of the pipe was ground off at the small section where there was contact between the parts. This is the second source of error mentioned above. The grinding of the pipe surface happened during the experiments, and changed the roughness of it throughout the experimental time. The surface roughness is very likely to have a major influence on the adhesive strength of a solid deposit, so the very first experiments should not be compared to the later experiments without any precautions.

As mentioned before, tetrahydrofuran is a chemical that easily evaporates when it's not in a closed container, which is the case in these experiments. The liquid mixture of THF and water was put in an open tank, so that some portion was likely to vaporize each test day.

At the end of a test day, a plastic bag was placed around the top of the tank so that it was almost completely sealed to reduce the loss of the liquid. The liquid loss that still happened, led to a change in the mixture proportion of the water and THF. This may have changed the whole mechanism of hydrate formation for the system, mainly regarding the induction time and the extent of hydrate formation (hydrate layer thickness).

During the implementation of experiments, it was observed that the temperature of the fluid in the tank had a relatively large variation through a typical test day. At the beginning of the day, the fluid would have approximately the same temperature as the surroundings, meaning 15 – 20 °C. As the cold fluid from the cooler was circulated through the pipe immersed in the tank fluid for several hours throughout the day, this would not surprisingly cool the tank fluid. The tank fluid temperature could be as low as 5 °C at the end of a test day. This would clearly affect the formation of ice and hydrate, and should have been considered at the start-up of the experiments when the testing procedure was formulated. This was not the case, meaning that two experimental results from different times of the day were not directly comparable, despite that every other parameter was identical. When the tank fluid temperature is low, ice and hydrate will form more easily since the liquid temperature is closer to the freezing temperature, and this causes a thicker deposit layer. As seen above, the strength of the deposit to the pipe is relatively dependent on the thickness of the deposit. The thickness depends on both the temperature of the cooling fluid, the no-touch time and the tank fluid temperature. Since the tank fluid temperature depends on the time of the day the experiments is conducted, or more accurately what test number of the day it has, the strength of the deposit is also indirectly dependent on this parameter.

A definite source of error in these experiments is that some of the equipment and equipment setup actually was changed during the experiment period. As explained previously, the mixture proportion of THF and H_2O changed with time, also changing the hydrate formation mechanism. The surface of the pipe was ground off, changing the properties of it. Glycol was added to the cooler a few times, altering its capability of reaching low temperature and the stability of the preset temperature. The large pressure inflicted on the pipe made it move a little bit, and also made it bend. This movement was the source of the skewness between the pipe and the scraper that is explained above. Due to this, a small piece of steel was placed between the horizontal section of the pipe and the flange to avoid it from happening. This was done after several experiments were already completed, possibly having a considerable impact on the rest of the experimental results. When the original steel pipe was changed into another pipe in order to find differences between them, the new pipe may have been placed differently than the first one. The scraper run remarkably easy up and down this pipe, and it is possible that it was fitted better in the equipment (regarding to the scraper) than the first pipe, making the relative difference between the two larger than it should have been. Another change that came with time was due to the fact that the rods used as the holder for the piston/ scraper were not made of stainless steel. The bottom part of the rods was immersed in the tank fluid, and therefore, it began rusting. The rust spread out in the liquid, and may have changed the chemical properties and mechanisms of it.

The cooler used in these experiments was a fairly simple one, equipped with a coil submerged into the cooling fluid. The coil would either heat or cool the fluid by the use of electric power. Due to the machines simplicity, it had some weaknesses regarding the stability

of the coolers temperature and also achieving the desired temperature. It was necessary to add glycol to the cooler fluid because it could not reach the temperature that was set. It was also seen that the machine had large challenges with keeping the lowest temperature (– 10 °C) for a longer period of time. At several occasions, especially when the no-touch time was 10 and 15 minutes, the cooler only held the temperature at – 10 °C for a few minutes, before it started to rise. At the end of the no-touch time, the temperature could be as high as – 8.5 °C, and this would undoubtedly have some influence on the hydrate formation and adhesive strength of it.

The pump that provided the pressure to push the piston down the pipe was also pretty basic. The handle on the pump was manually pushed up and down to move the oil in it through the hose to the piston in order to increase the pressure on it and make it move down the pipe. The handle obviously has a limited "span" from its starting position until it's pushed all the way down, and it was found that this span should be taken into consideration for the implementation of the pumping procedure. If the scraper was close to breaking through the hydrate layer but the handle was at the lower limit of its span, the handle needed to be pulled back up to start a new period. It was observed that in these cases, the pressure reading was often a bit higher than if the significant pressure build-up just before the breakage and the breakage itself both occurred in the same "span". A possible explanation for this is that when the pressure increase is not constant, the behavior of the hydrate will differ from one case to another. The hydrate gets a short time to "adjust" to the increased pressure, and may be compressed some before the pressure is increased again, meaning that it can withstand a little bit more pressure. The fact that the handle is pushed down by hand also gives a source of inaccuracy since the pressure increase is not constant during the whole span, and the rate the handle is pushed down will differ from experiment to experiment.

A rather surprising observation made during the experiment was that the hydrate formation sometimes was very different between the two sections at each side of the pipe holders. Both sides were submerged in the tank fluid, and other than the one section being a bit longer than the other, all parameters were the same, so there should be no differences between them. Nevertheless, hydrate formation sometimes occurred earlier on one side, while the other needed to be significantly triggered by making movements in the surrounding fluid and on the surface of the pipe section. This made differences between the hydrate layers on the two sides, mainly regarding the thickness. This difference is quite important since the measurement of the thickness was made on the opposite side from where the scraping was done. This could mean that the thickness readout made on the one side was very different from the actual thickness of the layer on the other side where the adhesive strength was measured.

During the whole time period of the experiments, it was seen that it got more and more difficult to start the formation of hydrate. The most probable explanation for this is the evaporation of THF from the tank fluid and the addition of rust in the fluid from the rods. Early in the testing, hydrate formation started almost immediately after – sometimes even before – the cooler had reached – 5 °C, and the no-touch time was started at once. But in later experiments, it often happened that no hydrate was made after several minutes with the temperature at – 5 °C. Stirring in the fluid sometimes helped, but not always. It was therefore found necessary to lower the temperature to – 7 or – 8 °C to trigger the formation to start, before it was raised back up to – 5 °C. This was also done for some of the experiments with

ice, where the temperature was set to – 5 °C to start formation of ice and then increased to – 4 °C which was the actual experimental temperature. This is clearly a source of error, both because this procedure was only used for some of the experiments and because the temperature of the experiment cannot be claimed to be precise.

4.3 Impact of the Parameters Tested

Aspenes et al. (2010) stated that some of the most important properties affecting the adhesion force between hydrates and solid surfaces are the surface material, presence of water and the contact time between the hydrate and the surface. In these experiments, four different parameters are tested, regarding the adhesive strength of hydrate deposits. These are the temperature of the cooler (and hence inside the steel pipe), the no-touch (or contact) time where the hydrate is left to grow, the thickness of the deposit and the surface properties of the solid surface (roughness, coating). Water is present in all the experiments, so all of aspects found to be important by Aspenes et al. are included through this work. Some results presenting all of the tested parameters are shown under "Results", and more can be seen in the Appendix. The impact of the cooler temperature is explained above, stating that a lower temperature gives a stronger adhesion between the hydrate and the solid surface. The no-touch time has also been discussed to some extent previously, and it was found that this has more of an indirect influence on the strength, given that the behavior of the system was not equal from experiment to experiment.

The thickness does however have a larger impact on the adhesion. A good example of this is seen in Figure 3.7. The relationship between the two parameters can be said to be close to proportional. One may automatically think that this is very logical; a thicker layer gives higher strength. But on further thought, the strength tested in this work is only the adhesive strength between the hydrate layer and the solid surface, so the only layer that should matter is the interface between the hydrate and the steel, and this has the same "thickness" in all experiments. The layer thickness should in other words not be very important, and still it clearly is. A thick layer will apparently increase the adhesion at the interface although only a small portion of it is in direct contact with the steel pipe. This, together with the finding that the no-touch time was not of great importance, may be partially explained by the work of Aman (2012, Ch.4). He found that the contact time between hydrate and solid surface had a large impact on the adhesion force, but only within a limited time period. From the first contact between the two substances, the contact time would be very important regarding hydrate nucleation at the surface. But after some time, the dominant mechanism changed from the nucleation to growth and so the layer thickness and growth rate played a larger role. This may explain that the thickness of the hydrate deposit is found to be more important than the no-touch time in these experiments.

The properties of the solid surface also turned out to have a significant impact on the adhesion. In Figure 3.6, the yellow, orange and green markers show the average pressure values for the experiments with the pipe with high roughness and the ones with the smoother pipe. It is easy to see that lower roughness leads to lower adhesion force. This result is in good agreement with the work done by Aman (2012, Ch.9.4), who found that a high surface roughness led to large adhesion forces, while smoother surfaces gave low adhesion. Nicholas

et al. (2009) on the other hand found through their experiments that the roughness did not have a significant impact, which strongly disagree with these results. The hydrate particles need a certain unevenness in the surface in order to be able to attach to it, so if the surface is perfectly slick, the particles won't have anything to "hold on" to, and it may not stick to it at all. Perfectly slick surfaces are rare, and often very expensive, so some level of roughness should be expected. The two coatings also changed the properties of the surface, and these changes include more than just the roughness. Both Baraka-Lokmane et al. (2014) and Akamine et al. (1992) found that the properties of the solid surface is one of the most important parameters when it comes to adhesion between an ice or hydrate particle and a solid surface. Coating a solid surface with a substance can change its wettability, the surface free energy, interfacial tension and heat capacity. There are no exact measures on these changes, only the pressure read-outs from the experiments. The purple and red markers in Figure 3.6 show the average values from these experiments, while Figure 3.9 and Figure 3.10 show the results in more detail. There is no clear difference between the two coatings, but the results does show that the pipe with high roughness gave lower adhesion force when coated with the automotive paint, while the smooth pipe got somewhat higher pressure readings when coated with the corrosion-avoiding primer. This last case still gave lower values than the rough pipe without coating.

An observation connected to the strength of the deposit was the relative difference in strength between the hydrate/ ice itself and the strength between pipe and deposit. As the piston reached the top of the deposit and the pressure was increased, it was seen that the deposit itself started to form cracks before any of it was scraped off of the pipe. The first of these cracks usually occurred at the horizontal section of the pipe, and then at the bend. This was merely a visual observation and there is no data to confirm it, other than the pictures seen in Figure 4.1**.** It is therefore not possible to draw a certain conclusion based on this, but it is a clear indication that the strength in the ice or hydrate itself is somewhat lower than the adhesive strength in the deposit on the pipe.

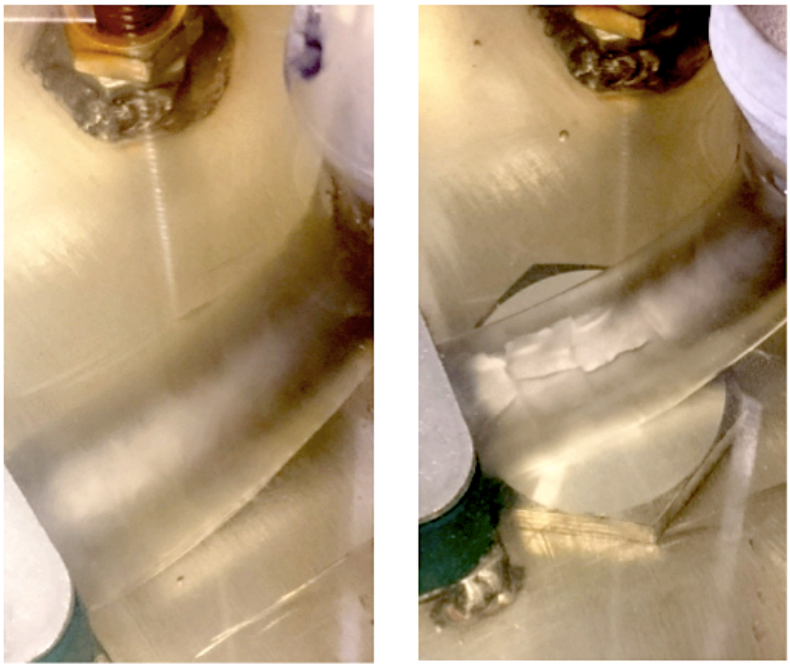

Figure 4.1: Pictures showing a hydrate deposit on the steel pipe right before (left) and right after (right) the pressure has been increased, but before any deposit has been scraped off of the pipe

A few other parameters are likely to affect the results of these experiments, but they have not been tested. As seen by Aspenes et al. (2010, 2009b), the wetting of the system and whether or not water is present, has a large influence on the adhesion. It was necessary to have liquid water present in all the experiments in this work, so it's hard to say how large influence it had. The system is expected to be water-wet, and it is very likely that the water has increased the adhesion compared to if the system only contained "dry" hydrate. If liquid water is present in addition to the water captured in the hydrate, it can easily make liquid bridges between these hydrate particles and the solid surface, and Aspenes et al. (2010) and Aman (2012) have shown that this can cause a significant adhesive force.

5 Conclusion and Recommendations

The results from the experiments done in this work showed that the different parameters tested have a different impact on the adhesion force of hydrate deposits. The temperature of the system clearly has an impact in that a lower temperature gives an increased adhesive force. The experiments is mainly done with petroleum production in mind, so a recommendation related to this finding is to take action to maintain the temperature of the petroleum at a high level in production lines. If the temperature is high enough, hydrate will not be formed at all and all problems related to it vanishes. If hydrate is formed but the temperature is kept at a relatively high level, the problems will be limited to a minimum and it is fairly easy to remove the deposit.

The thickness of the hydrate deposit was found to be one of the most influential parameters in this work, having a close to proportional relationship with the pressure needed for removal. The thickness of the layer is a function of both the temperature in the system and the time it is allowed to grow, so in order to restrict the growth, these other parameters also need to be considered.

The no-touch or growth time only has an indirect impact on the adhesion in that a long NTT often, but not always, leads to a large thickness. The consequence of a thick layer is explained above. Since the most widespread result of a long NTT is a thick layer of hydrate, the advice here is to deal with the problem as soon as possible by removing it, or at least try to limit the extent of the hydrate formation and growth.

The surface roughness of the solid surface was also found to have a significant importance regarding adhesion. A smooth surface makes it more difficult for the hydrate particles to attach to the surface, and this reduces the adhesive forces. A desired property for a petroleum-producing pipe should therefore be that the inner surface of the pipe is as smooth as possible.

6 Further Work

The experiments completed through this work were done with limited knowledge, time and resources. If experiments similar to these were to be done in the future, some recommendations and suggestions for this is given below.

- The container with hydrate former should be isolated from the surroundings to avoid evaporation. This will lead to a constant mixture proportion throughout the experiments, and the testing conditions are more similar for all of them.
- Actions should be made to make sure the equipment does not change or move during the experiments. In the experiments in this work, the coatings were worn off during the experiments, and the pipes were bent and misaligned, causing large inaccuracies.
- The tested coatings should also have been tested on the opposite pipes, i.e. the automotive paint on the smooth pipe and the primer on the rough pipe. To do this, the coatings already on the pipes would have to be removed from the pipes in a careful manner to avoid changes in the "clean" pipe surfaces.
- Other coatings, pipes with different roughness or pipes made of different materials would be very interesting to test. This could either verify the findings found in this work, or give completely different and new results and relationships.
- Other hydrate formers should also be tested to see if this gives other results regarding the deposit behavior.
- Testing at pressures and temperatures closer to actual operational conditions would be more valuable for the industry.
- The scraping mechanism and procedure can probably be done much more accurate.
- The length where the hydrate "break-off" happens should be measured so that the force can be calculated correctly.

7 Nomenclature & Abbreviations

α = *Angle of liquid bridge*
γ = *Interfacial tension*
γ_{so} = *Interfacial tension solid – oil*
γ_{sw} = *Interfacial tension solid – water*
γ_{wo} = *Interfacial tension water – oil*
θ = *Contact angle*
θ_c = *Wetting angle of liquid bridge*
θ_s = *External contact angle*
σ = *Surface tension*
χ = *Contact radius of liquid bridge*

A = *(Surface) Area*
AA = *Anti-agglomerant*
AP = *Automotive paint*
BC = *Base case*
CP = *Corrosion-avoiding primer*
d = *Immersion depth of particle in liquid bridge*
F = *Force*
F_A = *Cohesive force of capillary bridge*
f_{slv} = *Specific free energy at contact line between solid, liquid and vapor*
H = *Height of liquid bridge*
H_2O = *Water*
HET = *Hydrate equilibrium temperature*
KI = *Kinetic (hydrate) inhibitor*
LDHI = *Low dosage hydrate inhibitor*
MEG = *Monoethylene glycol*
NH_2 = *Amine*
NTT = *No-touch time*
OH = *Hydroxide*
P = *Pressure*
P_{avg} = *Average pressure-reading for one NTT*
P_{max} = *Maximum pressure-reading*
QLL = *Quasi-liquid layer*
R = *Radius*
R^* = *Harmonic mean radius*
R_1 = *Radius of particle 1*
R_2 = *Radius of particle 2*
RCE = *Rotating cylinder electrode*
SEM = *Scanning electron microscopy*
SP = *Smooth pipe*
THF = *Tetrahydrofuran*
THI = *Thermodynamic hydrate inhibitor*
W_{swo} = *Adhesion force solid – water with oil present*

8 References

Aarseth, F. (1997) 'Use of Electrical Power in Control of Wax and Hydrates', presented at *The 1997 Offshore Technology Conference,* Houston, Texas, USA, 1997, Offshore Technology Conference, 471-482

AK Steel Corporation (2007) *Product Data Sheet 316/ 316L Stainless Steel,* available at http://www.aksteel.com/pdf/markets_products/stainless/austenitic/316_316l_data_sheet.pdf (Accessed 13 Apr 2016)

Akamine, K., Matsuda, N., Takagaki, T. & Hirai, Y. (1992) 'Development and Actual Testing Results of Paint for Arctic Waters' in *Proceedings of the Second (1992) International Offshore and Polar Engineering Conference,* San Francisco, USA, 1992, ISOPE, 42-48

Aman, Z. M. (2012) *Interfacial Phenomena of Cyclopentane Hydrate.* PhD thesis, Colorado School of Mines, Golden (USA)

Aspenes, G., Dieker, L. E., Aman, Z. M., Høiland, S., Sum, A. K., Koh, C. A. & Sloan, E. D. (2010) 'Adhesion Force Between Cyclopentane Hydrates and Solid Surface Materials' in *Journal of Colloid and Interface Science,* 343 (2), 529-536

Aspenes, G., Høiland, S., Barth, T. & Askvik K. M. (2009b) 'The Influence of Petroleum Acids and Solid Surface Energy on Pipeline Wettability in Relation to Hydrate Deposition' in *Journal of Colloid and Interface Science,* 333, 533-539

Aspenes, G., Høiland, S., Borgund, A. & Barth, T. (2009a) 'Wettability of Petroleum Pipelines: Influence of Crude Oil and Pipeline Material in Relation to Hydrate Deposition' in *Energy & Fuels*, 24, 483-491

Baraka-Lokmane, S., Charpentier, T. V. J., Neville, A., Hurtevent, C., Ordonez-Varela, J-R., Møller Nielsen, F., Eroini, V., Olsen, J. H., Ellingsen, J. A. & Bache, Ø. (2014) 'Comparison of Characteristic of Anti-Scaling Coating for Subsurface Safety Valve for Use in Oil and Gas Industry', presented at *The International Petroleum Technology Conference,* Kuala Lumpur, Malaysia, 2014, IPTC

Kinnari, K., Hundseid, J., Li, X. & Askvik, K. M. (2014) 'Hydrate Management in Practice', in *Journal of Chemical & Engineering Data,* 60, 437-446

KRÜSS GmbH (n.d.) *Surface Free Energy,* available at: http://www.kruss.de/services/education-theory/glossary/surface-free-energy/ (Accessed 24 Feb 2016)

Larsen, R. (2014) *(Gasshydrat 1) Vann* [PowerPoint slides], lecture notes from the course 'TPG4135 – Processing of Petroleum' at the Norwegian University of Science and Technology, Trondheim

Larsen, R., Makogon, T. Y., Knight, C. A. & Sloan, E. D. Jr. (1997) 'Growth and Inhibition Phenomena of Single Hydrate Crystals' in *Preprints of Papers – American Chemical Society, Division of Fuel Chemistry,* 42 (2), 558-562

Liukkonen, S., Rytkönen, J., Alhimenko, A. & Kniazeva, E. (1997) 'On the Adhesion of Oil and Ice' in *International Journal of Offshore and Polar Engineering*, 7 (4), ISOPE, 246-253

Nicholas, J. W., Dieker, L. E., Sloan, E. D. & Koh, C. A. (2009) 'Assessing the Feasibility of Hydrate Deposition on Pipeline Walls – Adhesion Force measurements of Clathrate

Hydrate Particles on Carbon Steel' in *Journal of Colloid and Interface Science*, 331, 322-328

Sloan, E. D. & Koh, C. A. (2008) *Clathrate Hydrates of Natural Gases,* 3.edition, Florida: Taylor & Francis Group

Tracy, C. & Singh, R. (n.d.) *Heat Capacity*, available at http://chemwiki.ucdavis.edu/Core/Physical_Chemistry/Thermodynamics/Calorimetry/Heat_Capacity (Accessed 2 Mar 2016)

Usman, M. A., Olatunde, A. O., Adeosun, T. A. & Egwuenu, O. L. (2012) 'Hydrate Management Strategies in Subsea Oil and Gas Flowlines at Shut-in condition', in *Petroleum & Coal,* 54 (3), 191-202

9 Appendix

9.1 Risk Assessment

Since this master involved work in the lab, safety precautions needed to be taken. The student performing the lab experiments completed two different HSE courses (one from NTNU and one from SINTEF) online before any work in the lab started. A thorough tour of the lab including any potential hazards, first aid equipment and procedure for possible accidents and alarms was also conducted before the experiments began. Below is a table showing the specific dangers connected to these experiments and the actions taken to decrease the risk to a minimum.

Hazards	**Safety measures**
Experiments involving high pressure conducted in the same building	These were done in locked, confined safety chambers the student did not have access to during experiments
Gases and liquids in several readily available pipes inside the building, possible to change the pressure and temperature significantly	Instructions not to make any changes to the main systems in the building or the systems for each of the safety chambers
Chemicals harmful for people were present in the lab	These were enclosed in cabinets, with instructions for safety equipment and procedures that should be used when handling them
Tetrahydrofuran evaporates easily and the occurring gases can be harmful to people	The open tank with THF was placed in a partially open cell with an exhaust fan
Tetrahydrofuran and glycol are toxic and can cause harm to skin, eyes and so on	Use of safety glasses, gloves and lab coat at all times when approaching the equipment with the chemicals and avoiding ingestion
Pinch point hazard due to the piston/ scraper	Keep clear of the piston and scraper when the pressure was increased, carefully push it back up when the pressure had been removed
The cooler hose placed inside the scrapers slit could have loosened, releasing a significant amount of glycol to the surroundings, and hence possibly at people present	Regularly checking that the hose was securely fastened, that the scraper was not pushed too far up and wearing safety glasses when operating this equipment

Table 9.1: Possible hazards and the corresponding safety measures connected to the work in the lab

9.2 Additional Plots and Data from the Experiments

Ice - Pressure versus time					
Kset	**-5,00**	**Degrees Celcius**			
NTT [min]	**P0 [bar]**	**Pmax,read [bar]**	**Pmax [bar]**	**Pavg [bar]**	**Comment**
1	0,05	28,03	27,98	27,68	Very thin layer
1	0,05	29,60	29,55		Thin layer
1	0,06	25,56	25,50		
2	0,06	30,23	30,17	20,21	
2	0,03	24,34	24,31		
2	0,03	14,49	14,46		
2	0,03	11,93	11,90		
5	0,03	18,01	17,98	17,67	
5	0,01	14,06	14,05		
5	0,07	17,29	17,22		
5	0,04	26,07	26,03		Thicker layer
5	0,05	11,43	11,38		
5	0,03	23,54	23,51		Strong layer of frost
5	0,04	20,00	19,96		
5	0,05	12,19	12,14		
5	0,02	19,91	19,89		
5	0,06	14,55	14,49		
10	0,05	18,81	18,76	16,68	
10	0,03	21,20	21,17		
10	0,06	24,90	24,84		Thicker
10	0,07	18,85	18,78		Relatively thick
10	0,02	19,05	19,03		
10	0,06	11,17	11,11		
10	0,06	14,38	14,32		
10	0,09	14,93	14,84		
10	0,07	12,83	12,76		
10	0,10	11,30	11,20		
15	0,06	12,88	12,82	11,87	
15	0,05	11,03	10,98		
15	0,04	10,04	10,00		
15	0,07	13,74	13,67		
15	0,05	11,93	11,88		

Table 9.2: Data from experiments with ice at - 5 ^{o}C

Ice - Pressure versus time					
Kset	**-4,00**	**Degrees Celcius**			
NTT [min]	**P0 [bar]**	**Pmax,read [bar]**	**Pmax [bar]**	**Pavg [bar]**	**Comment**
2	0,01	7,08	7,07	8,38	
2	0,04	7,83	7,79		
2	0,08	10,56	10,48		
2	0,08	9,02	8,94		Not down to -5 first
2	0,04	7,66	7,62		Not down to -5 first
5	0,05	14,48	14,43	18,89	A bit thick at -5
5	0,05	18,22	18,17		Thin layer at -5
5	0,08	17,19	17,11		
5	0,06	20,46	20,40		Very thin at -5
5	0,08	23,88	23,80		Compression before breakage
5	0,05	19,48	19,43		
10	0,05	13,22	13,17	10,98	
10	0,14	11,67	11,53		
10	0,17	8,23	8,06		As good as no ice…
10	0,03	11,30	11,27		
10	0,06	10,95	10,89		

Table 9.3: Data from experiments with ice at - 4 ^{o}C

Hydrate - Pressure versus time					
Kset	**-5,00**	**Degrees Celcius**			
NTT [min]	**P0 [bar]**	**Pmax,read [bar]**	**Pmax [bar]**	**Pavg [bar]**	**Comment**
2	0,05	30,97	30,92	18,72	Equipment failure?
2	0,04	23,24	23,20		
2	0,04	6,90	6,86		Very thin
2	0,06	15,61	15,55		
2	0,08	17,17	17,09		
5	0,06	15,48	15,42	16,83	Thin layer at the upper part
5	0,06	17,31	17,25		
5	0,09	16,77	16,68		Thin layer
5	0,07	11,96	11,89		
5	0,09	19,49	19,40		Thin, almost no ice
5	0,05	16,71	16,66		
5	0,05	16,38	16,33		
5	0,04	18,78	18,74		
5	0,05	21,38	21,33		
5	0,05	14,66	14,61		
10	0,10	8,76	8,66	12,19	
10	0,07	10,43	10,36		
10	0,06	13,22	13,16		
10	0,08	16,42	16,34		
10	0,03	12,47	12,44		No sudden twitch/ jerk
10	0,04	18,28	18,24		
10	0,07	14,41	14,34		
10	0,07	6,84	6,77		Refill of THF and H2O
10	0,03	10,53	10,50		
10	0,08	12,12	12,04		
10	0,06	16,15	16,09		
10	0,06	7,45	7,39		
15	0,06	7,50	7,44	15,79	
15	0,08	16,86	16,78		
15	0,06	10,34	10,28		
15	0,07	21,71	21,64		
15	0,05	9,74	9,69		
15	0,07	11,05	10,98		
15	0,06	15,51	15,45		
15	0,05	24,78	24,73		
15	0,06	24,59	24,53		
15	0,05	16,39	16,34		

Table 9.4: Data from experiments with hydrate, base case at - 5 ^{o}C

Hydrate - Pressure versus time						
Kset	**-10,00**	**Degrees Celcius**				
NTT [min]	**P0 [bar]**	**Pmax,read [bar]**	**Pmax [bar]**	**Pavg [bar]**	**Thickness [mm]**	**Comment**
2	0,07	24,28	24,21	24,11		
2	0,09	23,67	23,58		4,00	
2	0,09	26,29	26,20		3,50	
2	0,08	22,59	22,51		3,50	
2	0,11	24,16	24,05			
5	0,08	27,38	27,30	26,25		Thick layer
5	0,03	24,60	24,57			
5	0,05	23,62	23,57			
5	0,05	25,87	25,82			
5	0,05	27,16	27,11			
5	0,05	30,89	30,84			
5	0,06	12,75	12,69			Thin layer, first of the day
5	0,07	25,46	25,39			
5	0,07	32,58	32,51			
5	0,05	32,75	32,70			
10	0,04	35,41	35,37	21,67		
10	0,05	38,98	38,93			Thick, very high reading
10	0,08	21,13	21,05			
10	0,07	27,64	27,57		4,50	
10	0,10	25,28	25,18			
10	0,08	5,64	5,56		2,00	Very thin
10	0,08	7,27	7,19		3,50	
10	0,08	12,27	12,19		4,00	
10	0,14	21,75	21,61		5,00	
10	0,07	22,14	22,07		5,00	
15	0,09	25,51	25,42	22,35	5,50	
15	0,08	21,06	20,98			
15	0,09	21,56	21,47		5,50	
15	0,08	21,98	21,90			
15	0,17	8,85	8,68		2,00	Thin layer, first of the day
15	0,11	20,98	20,87		4,50	
15	0,10	29,71	29,61		5,50	
15	0,09	25,12	25,03		6,00	
15	0,12	25,30	25,18		5,00	
15	0,09	24,48	24,39		6,50	

Table 9.5: Data from experiments with hydrate, base case at - 10 ^{o}C

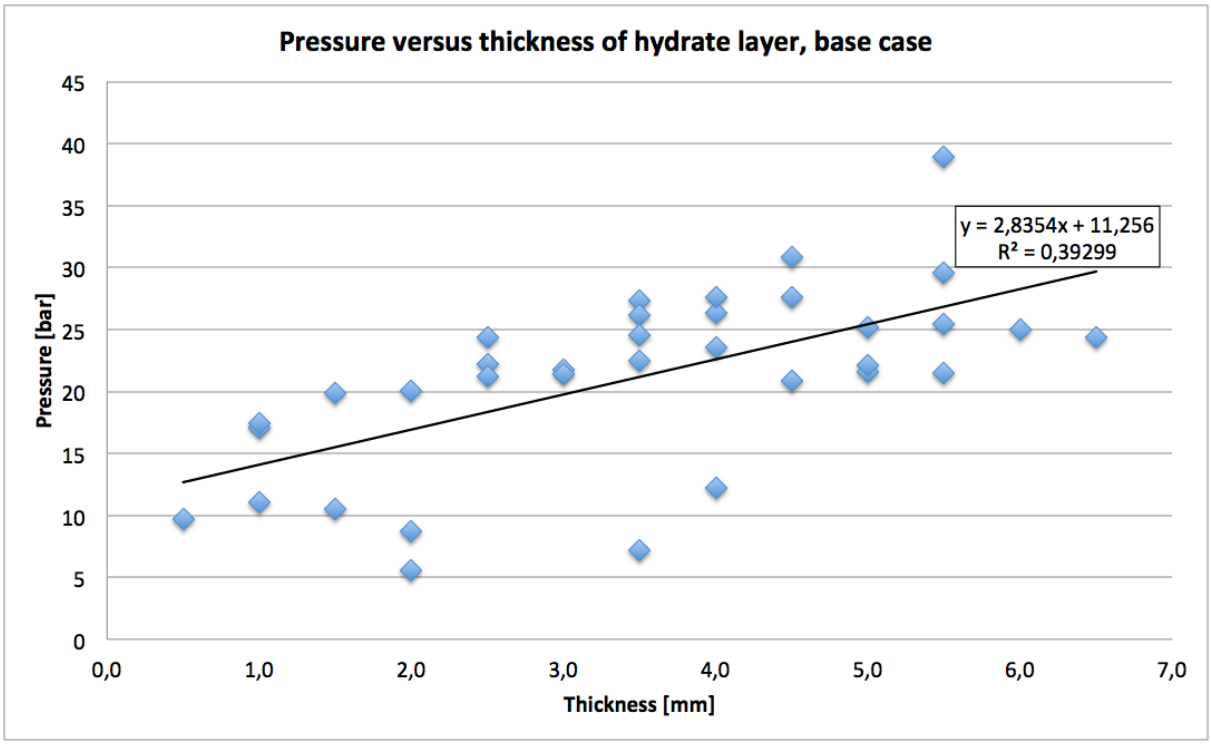

Figure 9.1: Plot of pressure versus thickness for experiments with hydrate, base case. A linear trendline with equation and how well it fits is included

Pressure versus thickness, BC	
Thickness [mm]	Pressure [bar]
3,5	27,3
4,5	30,84
5,5	38,93
4,5	27,57
2,0	5,56
3,5	7,19
4,0	12,19
5,0	21,61
5,0	22,07
5,5	25,42
5,5	21,47
2,0	8,68
4,5	20,87
5,5	29,61
6,0	25,03
5,0	25,18
6,5	24,39
4,0	23,58
3,5	26,2
3,5	22,51
1,0	17,09
0,5	9,67
1,0	17,47
1,0	11,04
1,5	19,83
2,0	20,03
3,0	21,73
2,5	22,22
3,0	21,42
3,5	24,56
2,5	21,17
4,0	26,32
1,5	10,55
2,5	24,37
4,0	27,61

Table 9.6: Data from experiments with hydrate, base case, measurements of thickness and pressure

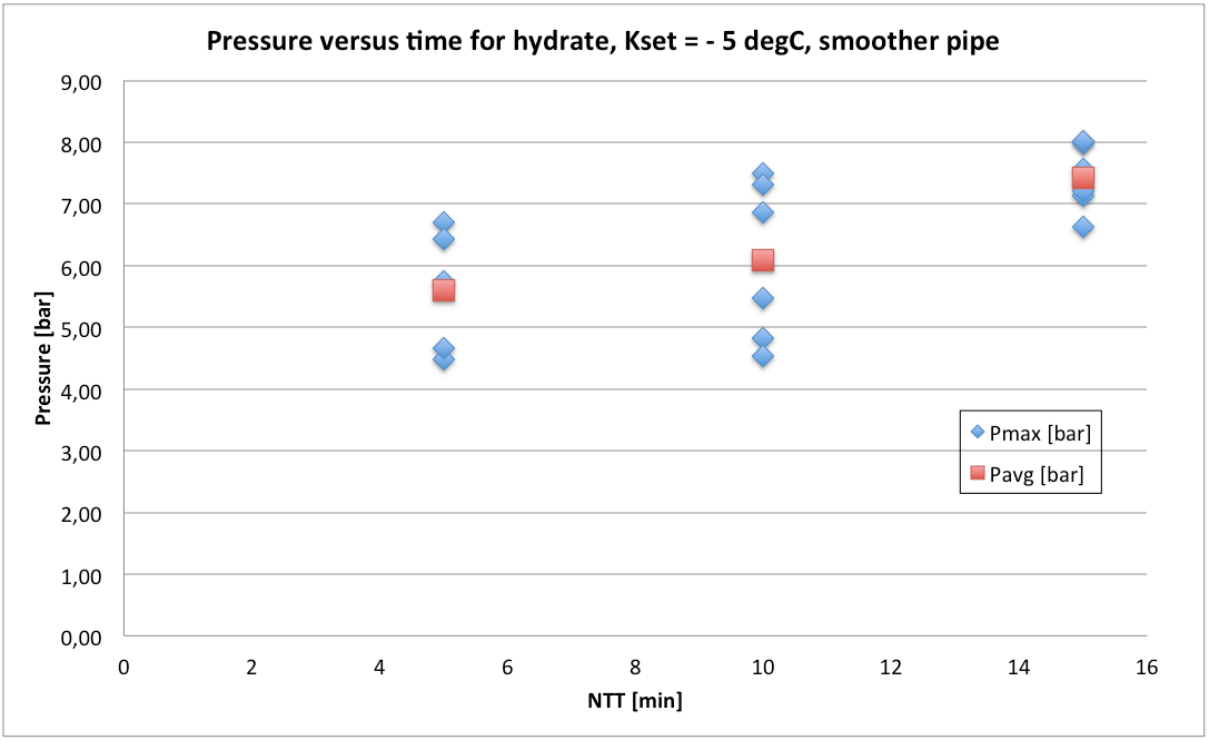

Figure 9.2: Plot of pressure versus no-touch time from experiments with hydrate, smoother pipe at - 5 °C

Hydrate - Pressure versus time, smoother pipe						
Kset	-5,00 Degrees Celcius					
NTT [min]	Thickness [mm]	P0 [bar]	Pmax,read [bar]	Pmax [bar]	Pavg [bar]	Comment
5	1,0	0,05	6,75	6,70	5,60	
5	1,0	0,04	4,52	4,48		
5	1,5	0,03	4,69	4,66		
5	2,0	0,04	6,47	6,43		
5	1,5	0,03	5,78	5,75		
10	2,0	0,08	6,95	6,87	6,08	
10	2,0	0,06	5,53	5,47		
10	1,5	0,03	7,53	7,50		
10	1,5	0,05	7,36	7,31		
10	1,5	0,05	4,87	4,82		
10		0,03	4,56	4,53		
15	3,0	0,05	7,18	7,13	7,43	
15	2,5	0,03	8,02	7,99		
15		0,04	6,67	6,63		
15	1,5	0,04	7,61	7,57		
15	2,0	0,03	8,05	8,02		
15	2,5	0,04	7,25	7,21		

Table 9.7: Data from experiments with hydrate, smoother pipe at - 5 °C

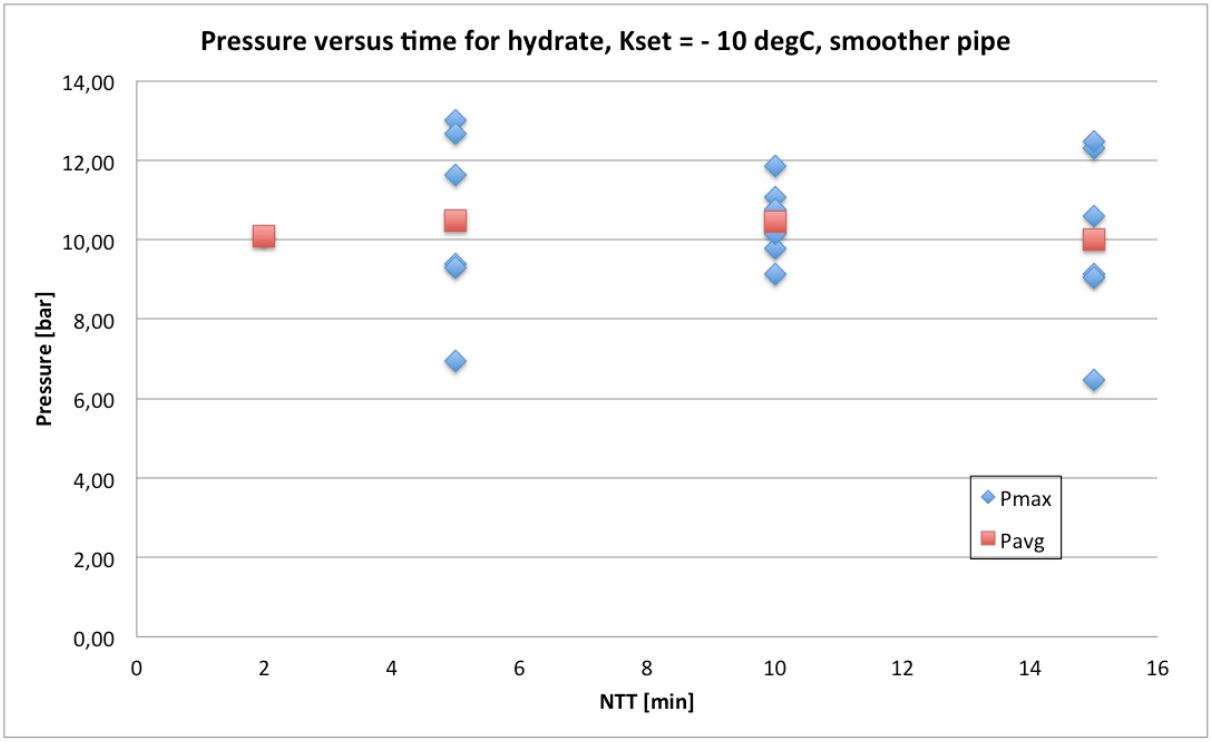

Figure 9.3: Plot of pressure versus no-touch time for experiments with hydrate, smoother pipe at - 10 °C

Hydrate - Pressure versus time, smoother pipe						
Kset	-10,00 Degrees Celcius					
NTT [min]	Thickness [mm]	P0 [bar]	Pmax,read [bar]	Pmax [bar]	Pavg [bar]	Comment
2	4,0	0,06	10,15	10,09	10,09	
5	5,0	0,07	13,07	13,00	10,49	
5	4,5	0,06	12,73	12,67		
5	5,0	0,06	11,70	11,64		
5	4,0	0,06	9,44	9,38		
5	4,5	0,05	9,35	9,30		
5	1,5	0,10	7,03	6,93		
10	3,0	0,04	9,17	9,13	10,46	
10	4,5	0,07	11,15	11,08		
10	5,5	0,06	11,92	11,86		
10	3,5	0,04	10,81	10,77		
10	4,5	0,05	9,83	9,78		
10	5,0	0,06	10,21	10,15		
15	2,5	0,05	9,19	9,14	10,00	
15	4,5	0,06	6,53	6,47		
15	5,5	0,06	12,36	12,30		
15	3,5	0,06	9,12	9,06		
15	4,5	0,05	10,63	10,58		
15	5,5	0,06	12,52	12,46		

Table 9.8: Data from experiments with hydrate, smoother pipe at - 10 °C

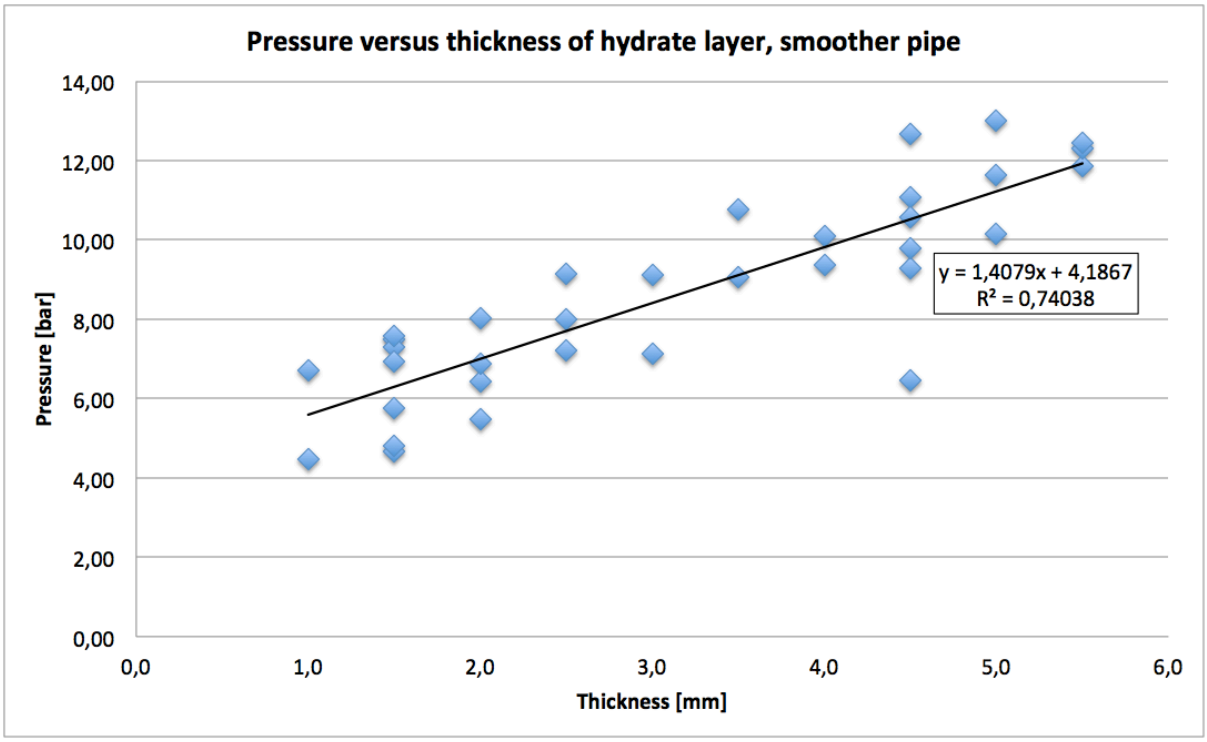

Figure 9.4: Plot of pressure versus thickness for experiments with hydrate, smoother pipe. A linear trendline with equation and how well it fits is included

Pressure versus thickness, smoother pipe			
Thickness [mm]	Pressure [bar]		
1,0	6,70		
1,0	4,48		
1,5	4,66		5 min
2,0	6,43		
1,5	5,75		
2,0	6,87		
2,0	5,47		
1,5	7,50	- 5 degC	10 min
1,5	7,31		
1,5	4,82		
3,0	7,13		
2,5	7,99		
1,5	7,57		15 min
2,0	8,02		
2,5	7,21		
4,0	10,09		
5,0	13,00		
4,5	12,67		
5,0	11,64		5 min
4,0	9,38		
4,5	9,30		
1,5	6,93		
3,0	9,13		
4,5	11,08		
5,5	11,86	- 10 degC	10 min
3,5	10,77		
4,5	9,78		
5,0	10,15		
2,5	9,14		
4,5	6,47		
5,5	12,30		15 min
3,5	9,06		
4,5	10,58		
5,5	12,46		

Table 9.9: Data from experiments with hydrate, smoother pipe, measurements of thickness and pressure

Hydrate - Pressure versus time, automotive paint						
Kset	-5,00 Degrees Celcius					
NTT [min]	Thickness [mm]	P0 [bar]	Pmax,read [bar]	Pmax [bar]	Pavg [bar]	Comment
2	2,5	0,03	19,57	19,54	19,54	
5	1,5	0,10	16,33	16,23	15,66	
5	2,0	0,09	11,36	11,27		
5	2,5	0,02	19,49	19,47		
10	2,5	0,07	18,67	18,60	14,71	
10	2,5	0,04	17,51	17,47		
10	1,0	0,06	6,88	6,82		
10	1,5	0,09	16,05	15,96		
15	3,0	0,08	19,84	19,76	15,77	
15	3,5	0,08	10,30	10,22		
15	3,5	0,10	17,44	17,34		

Table 9.10: Data from experiments with hydrate, automotive paint coating at - 5 ^{o}C

Hydrate - Pressure versus time, automotive paint						
Kset	-10,00 Degrees Celcius					
NTT [min]	Thickness [mm]	P0 [bar]	Pmax,read [bar]	Pmax [bar]	Pavg [bar]	Comment
2	2,0	0,06	19,09	19,03	19,03	Very slow down to hydrate
5	3,5	0,07	8,97	8,90	12,57	
5	4,0	0,07	13,51	13,44		
5	4,5	0,08	15,44	15,36		
10	2,0	0,07	6,71	6,64	8,63	
10	3,5	0,05	9,31	9,26		
10	4,5	0,09	9,54	9,45		
10	1,5	0,03	9,19	9,16		
15	6,0	0,05	14,65	14,60	15,80	
15	6,0	0,05	14,96	14,91		
15	6,5	0,06	17,94	17,88		

Table 9.11: Data from experiments with hydrate, automotive paint coating at - 10 ^{o}C

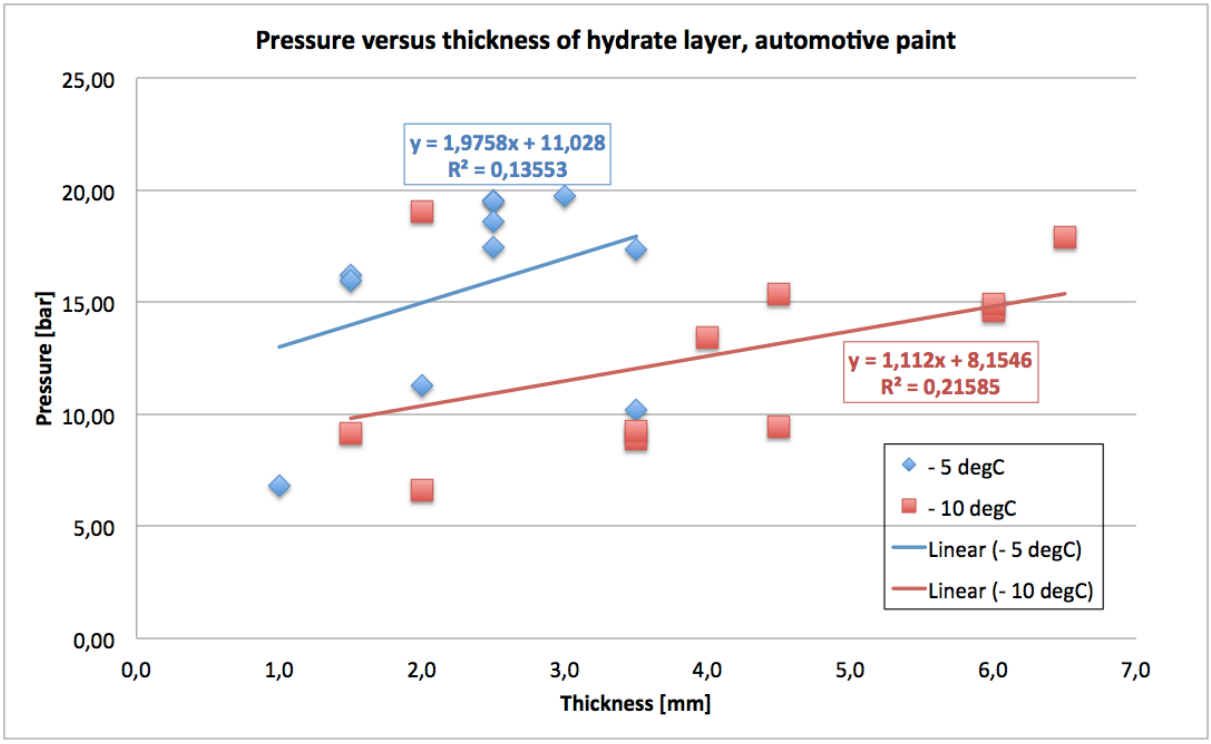

Figure 9.5: Plot of pressure versus thickness for experiments with hydrate, automotive paint coating. Linear trendlines with equations and how well they fit are included

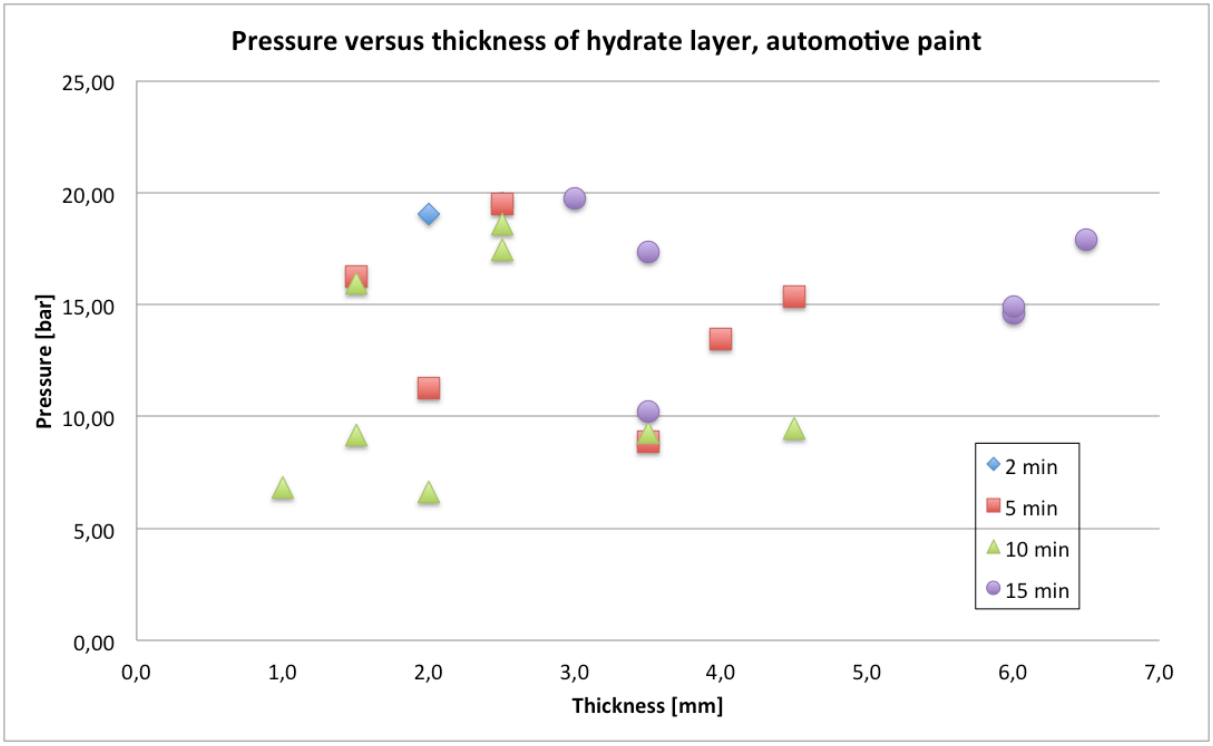

Figure 9.6: Plot of pressure versus thickness for experiments with hydrate, automotive paint coating, where the different no-touch times are seen

Pressure versus thickness, automotive paint			
Thickness [mm]	Pressure [bar]		
2,5	19,54	- 5 degC	2min
1,5	16,23		5 min
2,0	11,27		
2,5	19,47		
2,5	18,60		10 min
2,5	17,47		
1,0	6,82		
1,5	15,96		
3,0	19,76		15 min
3,5	10,22		
3,5	17,34		
2,0	19,03	- 10 degC	2min
3,5	8,90		5 min
4,0	13,44		
4,5	15,36		
2,0	6,64		10 min
3,5	9,26		
4,5	9,45		
1,5	9,16		
6,0	14,60		15 min
6,0	14,91		
6,5	17,88		

Table 9.12: Data from experiments with hydrate, automotive paint coating, measurements of thickness and pressure

Hydrate - Pressure versus time, corrosion-avoding primer						
Kset	-5,00 Degrees Celcius					
NTT [min]	Thickness [mm]	P0 [bar]	Pmax,read [bar]	Pmax [bar]	Pavg [bar]	Comment
5	1,5	0,07	7,40	7,33	7,03	
5	2,0	0,07	6,95	6,88		
5	1,0	0,04	6,92	6,88		
10	2,0	0,03	8,09	8,06	7,27	
10	1,0	0,06	6,29	6,23		
10	1,5	0,08	5,56	5,48		
10	2,5	0,08	9,37	9,29		
15	2,0	0,04	5,94	5,90	6,48	
15	2,5	0,07	6,33	6,26		
15	2,5	0,07	7,34	7,27		

Table 9.13: Data from experiments with hydrate, corrosion-avoiding primer coating at - 5 ^{o}C

Hydrate - Pressure versus time, corrosion-avoding primer						
Kset	-10,00 Degrees Celcius					
NTT [min]	Thickness [mm]	P0 [bar]	Pmax,read [bar]	Pmax [bar]	Pavg [bar]	Comment
2	3,0	0,05	14,21	14,16	14,16	
5	2,0	0,05	18,97	18,92	18,43	
5	3,0	0,06	24,02	23,96		
5	3,0	0,06	18,66	18,60		
5	4,0	0,04	12,28	12,24		
10	1,5	0,04	8,16	8,12	14,77	
10	3,0	0,06	18,07	18,01		
10	4,0	0,06	24,58	24,52		Very slow down to the hydrate
10		0,07	8,48	8,41		
15	5,0	0,06	23,08	23,02	20,79	
15	5,0	0,10	21,07	20,97		
15	5,0	0,06	18,45	18,39		

Table 9.14: Data from experiments with hydrate, corrosion-avoiding primer coating at - 10 °C

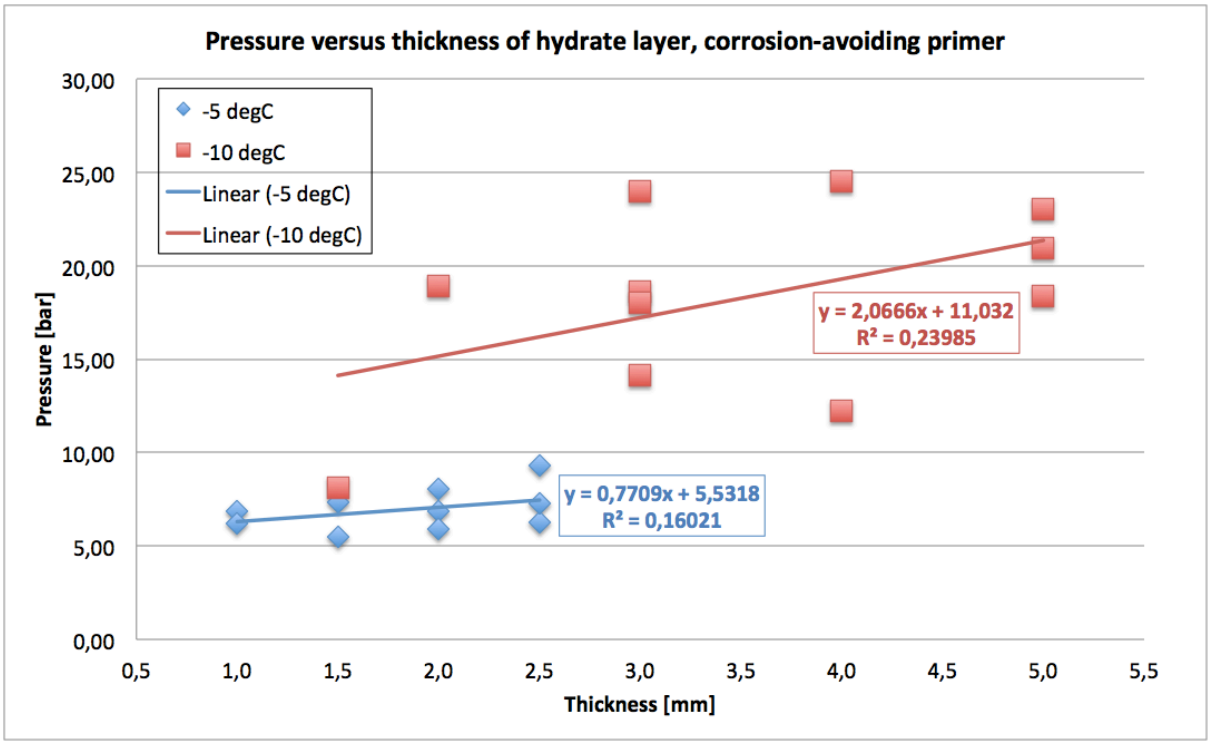

Figure 9.7: Plot of pressure versus thickness from experiments with hydrate, corrosion-avoiding primer coating. Linear trendlines with equations and how well they fit are included

Pressure versus thickness, corrosion-avoiding primer		
Thickness [mm]	Pressure [bar]	
1,5	7,33	- 5 degC
2,0	6,88	
1,0	6,88	
2,0	8,06	
1,0	6,23	
1,5	5,48	
2,5	9,29	
2,0	5,90	
2,5	6,26	
2,5	7,27	
3,0	14,16	- 10 degC
2,0	18,92	
3,0	23,96	
3,0	18,60	
4,0	12,24	
1,5	8,12	
3,0	18,01	
4,0	24,52	
5,0	23,02	
5,0	20,97	
5,0	18,39	

Table 9.15: Data from experiments with hydrate, corrosion-avoiding primer coating. Measurements of thickness and pressure